REVOLUTIONIZING SPACE PROPULSION THROUGH THE CHARACTERIZATION OF IODINE AS FUEL FOR HALL-EFFECT THRUSTERS

THESIS

Adam C. Hillier, Second Lieutenant, USAF

AFIT/GA/ENY/11-M08

DEPARTMENT OF THE AIR FORCE
AIR UNIVERSITY

AIR FORCE INSTITUTE OF TECHNOLOGY

Wright-Patterson Air Force Base, Ohio

AFIT/GA/ENY/11-M08

REVOLUTIONIZING SPACE PROPULSION THROUGH THE CHARACTERIZATION OF IODINE AS FUEL FOR HALL-EFFECT THRUSTERS

THESIS

Presented to the Faculty

Department of Aeronautics and Astronautics

Graduate School of Engineering and Management

Air Force Institute of Technology

Air University

Air Education and Training Command

In Partial Fulfillment of the Requirements for the

Degree of Master of Science in Astronautical Engineering

Adam C. Hillier, BS

Second Lieutenant, USAF

March 2011

AFIT/GA/ENY/11-M08

REVOLUTIONIZING SPACE PROPULSION THROUGH THE CHARACTERIZATION OF IODINE AS FUEL FOR HALL-EFFECT THRUSTERS

Adam C. Hillier, BS

Second Lieutenant, USAF

March 2011

Approved:

_____	_____
LtCol Richard E. Huffman, Jr. (Chairman)	Date
_____	_____
Dr. William A. Hargus, Jr. (Member)	Date
_____	_____
LtCol Richard D. Branam (Member)	Date
_____	_____
LtCol Carl R. Hartsfield (Member)	Date

Abstract

The demand for increased performance in space propulsion systems is higher than ever as missions are becoming more advanced. As the global supply of xenon depletes, missions demanding high thrust will require alternatives. The research presented here examines iodine as an alternate propellant. The propellant was successfully operated through a BHT-200 thruster in the T6 vacuum facility at Busek Co. Inc. A feed system for the iodine was developed for controlled thruster operation at varying conditions. An inverted pendulum was used to take thrust measurements. Thrust to power ratio, anode efficiency, and specific impulse were calculated. Iodine performance is compared to xenon. Plume measurements were taken by a nude Faraday probe, which measured current density, and an ExB probe, also known as a Wein filter, which measured individual species properties. The data validated anode efficiency from performance measurements. Plume comparisons were made between iodine and xenon. Iodine was found to perform similarly to xenon, but with superior performance at high voltage. Possible effects of iodine operation on spacecraft, thrusters, and power systems were explored.

Acknowledgements

If you helped… you know…

Table of Contents

Page

Page

List of Figures

Page

Page

List of Tables

Page

List of Symbols

α	=	multiple ionization correction factor
η_b	=	beam current efficiency
η_T	=	total efficiency
η_m	=	utilization efficiency
e	=	charge of an electron
F_t	=	thrust divergence factor
γ	=	current efficiency
g	=	gravitational acceleceration at sea level
I_b	=	propellant current flow
I_d	=	discharge current
I_i	=	ion current
I^+	=	current of singly ionized ions
I^{++}	=	current of doubly ionized ions
Isp	=	specific impulse
j_b	=	current density
$j(\theta)$	=	current density as a function of angle off thruster centerline
M	=	mass of a discharge ion
P_T	=	total power
P_d	=	discharge power
P_k	=	keeper power
P_{mag}	=	electromagnet power
r	=	radial distance from center axis
T	=	thrust
θ	=	angle off thruster centerline
V_b	=	exit voltage potential
V_d	=	discharge voltage potential
ϕ	=	ExB sweep voltage
ζ_{i}	=	ion mole fraction
Ω_{i}	=	ion current fraction

CHARACTERIZATION OF IODINE FUELED HALL-EFFECT THRUSTERS

I. Introduction

Propulsion systems are an essential subsystem on space vehicles. This research attempts to not only improve these systems, but create a more diverse arsenal of propulsion options. It is the goal of this chapter to provide motivation for improving propulsion technology. This chapter will also identify the objectives of the research and how to accomplish them.

I.1 Motivation

Cost, performance, and efficiency are the key factors in any engineering undertaking. It is an ongoing struggle to increase all three in any engineering discipline. In the field of space propulsion, the need for increased performance and efficiency is paramount as the effects are amplified greatly. Traditionally, propulsion efficiency refers to mass efficiency. Mass efficiency refers to how well a given mass changes the velocity of a spacecraft. The less propellant mass needed to maintain or change orbits in space, the more payload mass is able to be on orbit. This leads to less cost for space missions being flown. Another efficiency is electrical efficiency, which is specific to electric propulsion. Higher electric efficiency relaxes the requirements of the power subsystem, which also decreases mass and cost of a satellite. These gains motivate the industry to find better, more efficient propulsion systems.

The demand for more aggressive space missions is ever increasing. Many of these missions demand mass efficient propulsion systems powerful enough to both maintain orbits and propel interplanetary satellites. Additionally, with the increasing

amount of Earth satellites on orbit, the need for more precise station keeping is becoming dangerously apparent. This is particularly true in the case of geosynchronous satellites, which are not perfectly stable. Geosynchronous satellites are being packed in closer to each other. The small amount of drift inherent in nearly all geosynchronous orbits must be precisely countered to prevent these satellites from colliding. To do so, requires constant updates to orbital velocity. Also, these satellites are built to endure longer than a typical low Earth orbiting satellite. This is because there is no notable air drag at this altitude, and the satellites are enormously more expensive to put on orbit. Therefore, the orbital maneuvers needed to correct position and velocity are not only frequent but are required over a long period of time. Such updates add up to a substantial load on the propulsion system. Electric propulsion systems answer this demand with high performance and high efficiency.

Chemical propulsion, even at its theoretical maximum, is inadequate for the future of space propulsion. Humble et al. comment “Of the various methods for generating high speed reaction-mass, electromagnetic techniques offer the only way that, in principle, is not limited by the bond strengths of matter” [1]. Electric propulsion provides more reasonable solutions to the space propulsion missions. Humble et al. go on to describe electric propulsion theory: “In electric propulsion systems, electromagnetic forces directly accelerate the reaction-mass, so we are theoretically limited only by our ability to apply these forces at the desired total power levels” [1] . Mass efficiency is highly increased in electric propulsion systems due to this method of acceleration, the degree of which is determined by the type of electric system being used.

The Hall-effect thruster currently provides a promising solution to getting high enough mass efficiency for future space systems. Of all the electric propulsion systems, the Hall thruster is practical for its high power to thrust ratio and its efficiency.

The Hall thruster was used mainly by the former Soviet Union over the last several decades, but has become more popular all over the world in the last two decades [1]. Russian development proved Hall thrusters can provide the necessary efficiency and performance of many future space missions.

The SPT-100 shown in Figure 1 is a good example of a Hall thruster currently in use. This thruster is manufactured in Russia by Fakel. The Hall thruster is a proven electric propulsion system but still has room for improvement [1]. Among the potential improvements is the propellant choice.

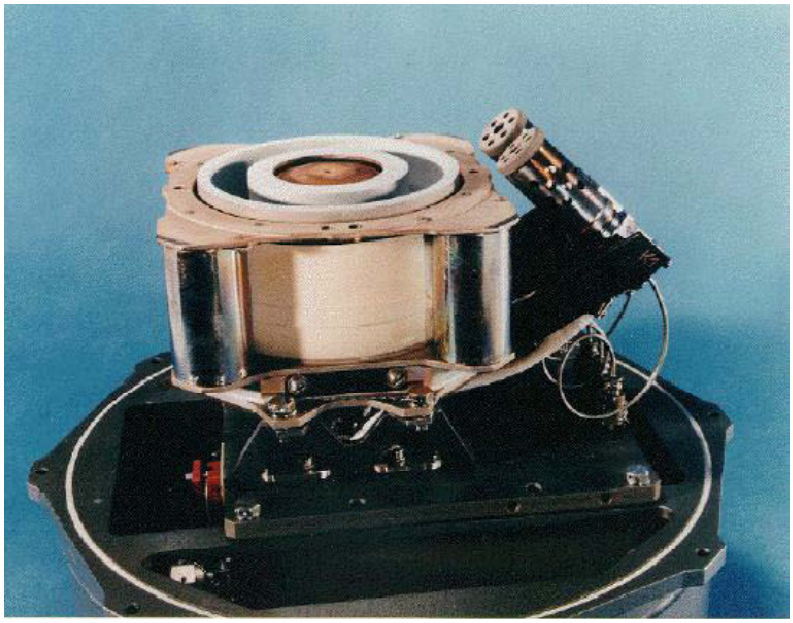

Figure 1: Fakel SPT-100 Hall Thruster, taken from astronautix.com [2]

Hall thrusters typically use gaseous propellants like xenon to produce thrust. Many other types of propellants are hypothesized for Hall thruster applications. There

are several untested propellants with the potential to be higher performing. This could increase performance, increase efficiency, and lower the cost of Hall thruster systems.

I.2 Problem Statement

Typically in a Hall-effect thruster, propellants are gaseous at room temperature because no heating or cooling is required before the fuel is converted to plasma inside the thruster. In addition, these propellants are often inert. This is advantageous as they do not interfere with the thruster itself. The optimal gaseous propellant for most applications has a high molecular weight in order to increase both thrust and electrical efficiency. This leaves a short list of propellant choices, usually resulting in one of the heavier noble gases like xenon. However, non-gaseous elements will typically ionize more readily than the noble gases. The ionization potential is a measure of how easily a species ionizes. Not limiting choices to the stereotypical noble gases results in a myriad of interesting propellant choices, many of which can outperform xenon in nearly every category.

Iodine is a particularly interesting choice as a propellant since it is almost as heavy as xenon, the heaviest of the stable noble gases, and it is easier to ionize than xenon. Other alternatives to the noble gases are metals. When these metals are ionized and ejected from a Hall thruster, they sometimes return to the spacecraft. This can result in plating of important hardware. Iodine, a non-metal, does not introduce the plating problems present in a metal propellant fueled Hall thruster. However, iodine introduces an oxidation issue. Iodine, being more fairly electronegative, may oxidize certain materials. This can be more or less of a problem than plating, depending on the hardware of the spacecraft. Iodine can be vaporized using less power than most other propellants.

Several prospective propellants have significantly high melting points, which would need to be overcome before it can be flowed through a feed system and converted to plasma. The melting point of iodine is one of the lowest of the alternate propellant options. Finally, cost is another important factor. Xenon is a very expensive substance and is not produced in high quantity. As of 2001, roughly ten tons per year of xenon was produced [3]. This could not sustain terrestrial industry and future space systems. The future of space depends on a more readily available propellant and one that is not going to dominate costs. Iodine is much cheaper than its noble gas counterpart xenon. This is mainly because iodine is 25,000 times more abundant in the Earth's crust [4]. Iodine is a good alternative, but using it has its own technical barriers. One major barrier is its state of matter at room temperature.

Iodine, being a solid at room temperature, cannot be simply injected into the combustion chamber. The complexity in designing thrusters to use Iodine as a fuel acts as a barrier to this technology moving forward. The technology has been developed to adequately vaporize and pump solid propellants. However, integration is not fully tested to the point of confidently operating iodine propellant Hall thrusters while maintaining the proper storage temperature. This is an engineering issue for operating these thrusters. Although iodine may produce favorable theoretical results, the amount of power needed to sustain the gaseous iodine must be considered. Including this in the power to thrust calculations more accurately relates current systems with possible iodine replacements [4].

An additional technical barrier is that iodine is not ideal in terms of ionization. Other species have better ionization characteristics. Metals typically will be influenced

by a colliding electron to release an electron of their own and become positively charged ions. Because iodine is more commonly a negative ion, at least in the monatomic state, it is possible that an interaction with an electron could influence the diatomic iodine to disassociate and create a negative ion. This would hurt the performance and efficiency of the thruster as the electric field is meant to accelerate positive charges to produce thrust [4].

Since iodine injected thrusters are more difficult to build, operate, and maintain, the profiles of these thrusters is not yet well understood. The exhaust profile needs to be well characterized before an iodine fueled system can be flown in actual missions. More data must be collected to prove iodine as a viable option as a fuel. Unfortunately, there are complications to testing the iodine propellant. The iodine plasma is more difficult to measure as it is more likely to corrode intrusive measuring devices. Many intrusive probes would be preferable to get the best experimental data possible, but their degradation can skew results and ruin equipment. Other types of instrumentation must be used in order to adequately characterize the entire exhaust profile [4].

I.3 Research Objectives

The objective of this research is to build and operate an iodine fueled Hall thruster. Optimally, the research should fully characterize the iodine thruster at as many operating conditions as possible. These characterizations would include thrust, specific impulse, and efficiency. The exhaust plume of the thruster will be measured to better understand the mechanisms of iodine operation and to compare efficiency to the performance measurements. The data will address the feasibility of using iodine as a

propellant in future thrusters. Xenon will also be used as a baseline for comparison at all iodine conditions. The research will attempt to address all concerns about running iodine in a Hall thruster from the feed system to the component limitations.

The research will use a 200 Watt Hall thruster designed by Busek with iodine as a propellant. Data from the exhaust will be measured by a non-intrusive probe. The data will be compared to the same thruster's data with xenon as a propellant. Similar power and mass flow numbers will be used to minimize variables in the problem.

The research will show whether the iodine can successfully be converted to a gas, ionized, and accelerated by the thruster. When the performance is measured, the data will dictate whether the efficiency and/or thrust to power ratio increases or not. The overarching goal will be to determine the overall viability of the technology. It is not yet known if iodine is even usable as a propellant, and this research will be able to answer that.

II. Theory and Previous Research

The goal of this chapter is to discuss Hall thruster applications and operation. An in-depth look at the Hall thruster physics helps compare iodine propellant to other propellants, like xenon. This is done by using the physical properties of the propellants and applying them to the equations governing thruster operation. Common performance characteristics serve to compare the propellants. Finally, the chapter discusses instrumentation with the ability to measure the desired performance characteristics.

II.1 Hall Thruster Applications

Hall thrusters have been around for decades. However, they have limited flight time aboard operational satellites. Prior to 1990 the West did not use Hall thrusters for any practical purpose [5]. Now, these systems are being flown aboard operational satellites. Today Hall thrusters are commonly used for station keeping of satellites. Geosynchronous satellites are the main use of this propulsion system but there are certainly others.

Hall thruster performance varies a great deal with design. Thrust generated is in the milli-Newton range for low thrust applications and in the Newton range for high thrust applications. Peak specific impulse ranges from 1,100 sec to 3,000 sec and higher [1, 6]. Design point thrust efficiencies are typically 30% to 70%. The input power of the thruster drives these numbers. Power acts as the scaling up factor for electric propulsion systems. More power input to a Hall thruster can easily drive Isps higher than 3,000 seconds and thrust above one Newton. Efficiency is partially dictated by this power as well, but theoretical limitations also come into play.

Ion engines are a competitor with Hall thrusters. Ion engines typically will have higher Isps. This makes them more practical for missions requiring a lot of velocity change over the long periods. However, in low power applications, a Hall thruster will typically have lighter components than the ion engine designed to accomplish the same mission [1]. This can make the Hall thruster a better engineering choice depending on the requirements. Also, time is a deciding factor in some missions. For example, an engine that is 100 times more mass efficient may take 100 times longer to reach the desired destination. Travel time becomes even more important when talking about interplanetary missions, especially manned missions. Since Hall thrusters will generally produce higher thrust than a comparable Ion engine, the Hall thruster will maneuver a spacecraft more quickly, thus reaching the desired velocity in less time [7].

II.2 Hall Thruster Theory of Operation

Hall thrusters are an electric propulsion system. This means that thrust is generated is due to the transfer of electrical energy to particle kinetic energy. There are several means of accomplishing this. Hall thrusters are typically categorized as an electromagnetic thruster, although it is more of a hybrid of two different types. Electromagnetic specifically means the particle velocity is achieved by the use of interacting electric and magnetic fields. The Hall thruster makes use of the electrostatic force to accelerate a charged particle out of the exhaust. Many other electric propulsion systems also use the electrostatic force to produce thrust, but they all operate differently.

The Hall thruster's geometry and thrust mechanism make it unique. A Hall thruster consists of an annular channel with the inner faceplate being an anode. Both the

inner and outer cylinders are fitted with electromagnets facing the channel. The magnets produce a uniform radial magnetic field. A cathode is generally fitted somewhere outside of the channel. This cathode will emit electrons. By the electrostatic force, these electrons will be attracted to the positively charged anode. This flow of electrons creates an electric field along the axial direction. As the electrons enter the channel, they will be captured by the interacting electric and magnetic fields into a swirling motion. This flow of electrons is referred to as the *Hall current*, from which the Hall thruster is named.

The electrons are swirling not only around the center axis of the Hall thruster, but they are also making small loops around the magnetic field lines. This means that the electrons will be moving axially in a periodic motion. The radius of this second type of circular motion is known as the Larmor radius and is given by;

$$r_L = \frac{v_\perp}{\omega_c} = \frac{1}{B}\sqrt{\frac{2mV_\perp}{e}} \tag{1}$$

where $v_\perp$ is the velocity perpendicular to the radial magnetic field lines,ω_c is the cyclotron frequency, $V_\perp$ is the perpendicular voltage, and B is the magnetic field strength. The corresponding azimuthal drift velocity is given by;

$$\boldsymbol{v} = \frac{\boldsymbol{E}\times\boldsymbol{B}}{B^2} \tag{2}$$

where **E** and **B** are the vectors for electric field and magnetic field respectively. The electron Larmor radius sizing is used to size the depth of the Hall thruster's channel. The radius gives the radius at which an electron will turn once it is introduced to the radial magnetic field lines. In a Hall thruster, this radius will describe how the electron will turn from moving axially toward the anode, to swirling around the center. It is important to be sure the electrons are properly introduced into the swirling flow and do not go

directly to the anode. If they are properly turned, they can then ionize the propellant as it enters.

As the electrons are swirling steadily around in the channel, a propellant can then be injected through the anode. Typically, a gas is introduced into the swirling Hall current where it is ionized by the electrons. Once the ionization occurs, the newly formed positive ion and electron will both be influenced by the strong electric field discussed above. The positive ion will begin to move out of the thruster, while the electron will move into it. The positive ion is much heavier than the electron, so the magnetic field's ability to turn the ion will be small. Once the ion has exited the thruster's channel, it is then neutralized by the electron beam coming from the cathode. This neutralizing of the plume keeps the ion from returning to the thruster due to the electric field as well as reduces the overall change in charge on the thruster [8].

Figure 2 illustrates a typical cross section of a Hall thruster. It is important to realize that this is the cross section of a torus like object. The upper and lower channels are actually physically connected in three dimensions. The electrons are moving out of the paper on the top side and into the paper on the bottom, resulting in a counter-clockwise swirling as viewed from the exhaust plume. The electron current originates from the cathode. Some of the electrons enter the channel creating the Hall current while others neutralize the plume. The channel electrons collide with neutrals creating ions, which are accelerated along the electric field lines.

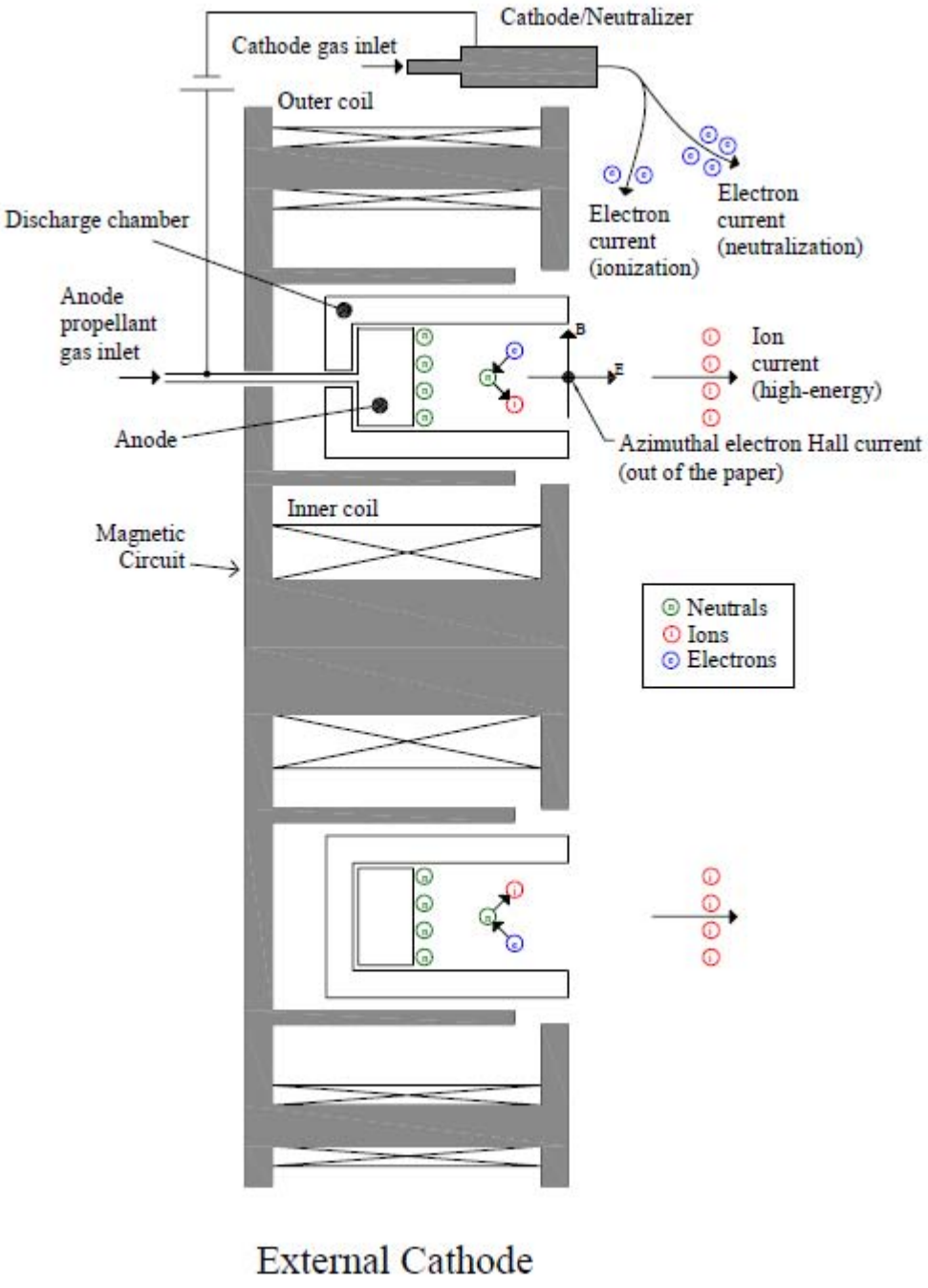

Figure 2: Cross section of a Hall thruster with an externally mounted cathode, taken from Hofer et al. [9]

II.3 Hall Thruster Propellants

Many propellants have been theorized for Hall thrusters. However, few are actually being used operationally in the space industry. Some propellants are not used due to technical challenges specific to the propellant. Other propellants have not been adequately researched. Some examples of Hall thruster propellants include bismuth, zinc, krypton, iodine, cesium, cadmium, and mercury, each with its own list of advantages and disadvantages. Table 1 lists several properties for each of the potential propellants. Each of the listed properties is important for estimating performance. The melting and boiling points are a measure of how easily the species will vaporize and flow through the thruster. The lower temperatures are less challenging to achieve. The ionization energy is related to efficiency. Typically, lower ionization energies translate to higher efficiency, particularly at low discharge voltages. The atomic mass affects all the performance characteristics. Thrust increases with higher atomic mass, while specific impulse decreases. Finally, cost is displayed as a measure of feasibility for the propellant.

Table 1: Properties of selected Hall thruster propellants, taken from Massey and King [10]

Propellant	Melting Point (C)	Boiling Point (C)	Ionization Energy (eV)	Atomic Mass (amu)	Cost Per kg in 2005
Bismuth (Bi)	271	1559	7.3	209	$6
Cadmium (Cd)	321	765	9	112.4	$25
Cesium (Cs)	29	685	3.9	132.9	$40,000
Iodine (I)	113	182	10.4	126.9	$484
Krypton (Kr)	NA	NA	14	83.8	$295
Mercury (Hg)	-39	357	10.4	200.6	$4
Xenon (Xe)	NA	NA	12.1	131.3	$1,138

Combining the data in Table 1 with thruster operating conditions gives reasonable estimates of thruster performance parameters, like thrust. Thrust is one of the major performance parameters when picking a system. The equation for thrust in a Hall thruster is given by:

$$T = \sqrt{\frac{2MV_b}{e}} I_b \tag{3}$$

where I_b is the current flow of the propellant, V_b is the voltage potential across the exit, and M is the atomic mass of the propellant [8, 11]. Current flow and voltage are directly proportional to the power output of the thruster itself. Therefore, a good first order assumption when comparing propellants for a given thruster is that the current and voltage are both approximately constant. If the assumption is valid, then thrust will increase for propellants with higher atomic mass numbers. Bismuth would be the highest thrusting propellant of those shown above.

The first order approximation breaks down when propellants are more easily ionized than other propellants. For example, iodine is more easily ionized than xenon. This can be seen in Table 1 in the ionization potential. Lower ionization potential means that less energy is needed to induce ionization. Further evidence is shown in Figure 3. The ionization cross section corresponds directly to probability of an atom being ionized. Iodine is clearly more likely to be ionized than xenon at electron energies between 10eV and 200eV. This means for a given power setting, more iodine will be ionized and flow out the exhaust. This is directly related to current flow. Increasing current flow directly increases thrust. If xenon and iodine have very similar molecular masses and iodine is

more likely to ionize, then thrust would be increased overall in an iodine propellant system.

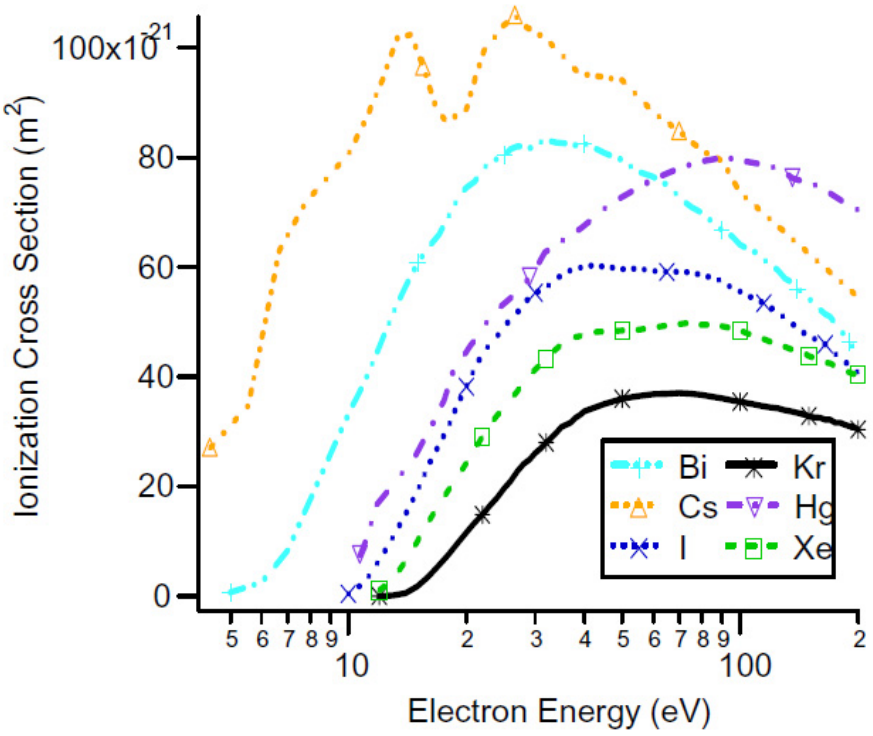

Figure 3: Ionization cross sections for various Hall thruster propellants, taken from Kieckhafer and King [3]

Another important effect of using iodine specifically is that it can ionize as a diatom, making the propellant atomic mass nearly 254 amu. This is not going to happen in 100% of the ionizations, but it may turn out to be more common than the dissociation case. It only takes 9.4 eV to ionize the diatomic iodine, while 10.4 eV is required for the monatomic iodine [4]. This does not consider the 1.5 eV needed to dissociate the iodine in the first place. If dissociation energy is considered, then the case of monatomic ionization is even less likely than the diatomic ionization. The diatomic iodine could outperform bismuth in terms of thrust. The experiments should show some increase in

thrust over the theoretical monatomic case because the mixture of diatomic and monotomic iodine will have a higher atomic mass than the uniform mixture of monatomic iodine [4].

On the other hand, iodine may have trouble producing thrust at all. Iodine is one of the halogens, which means it has a tendency to become a negative ion. The electro negativity describes the amount of energy needed for the monatomic or diatomic iodine to capture an electron. The electro negativity of iodine is 2.5 eV for the diatomic and 3.0 eV for the monatomic species. This is a low number compared to the ionization energies. It is possible for the iodine in the plasma to capture electrons and become negative ions. These negative ions would be forced to move in the same direction as the electrons: into the thruster. The negative ions would not be captured into a swirling motion like the electrons because the force on the charged particle would be the same as an electron. The same force on a more massive particle would not turn it enough. This means the negative ions would likely head directly for the anode. Obviously this would be undesirable from a thruster standpoint. One possible reason for this not occurring may be found in the energy of the electrons influencing ionization. The electrons are traveling with more energy than the electron affinity of iodine. These electrons could have too much energy to be captured. The last possibility suggests the iodine will only be able to capture some of the less energetic electrons, resulting in a low probability of negative ionization. Experimentation is needed to show which process is dominant. For these reasons, the potential exists for a superior thrusting system. Iodine can outperform the conventional xenon thruster if the conditions are right. The thrust is not the only important characteristic. Specific impulse is equally essential to achieve superior performance.

Specific impulse is another measure of performance that must be considered between the propellants. The specific impulse, or Isp, is given by:

$$Isp = \frac{\gamma \eta_m}{g} \sqrt{\frac{2eV_b}{M}} \tag{4}$$

where γ and η_m are efficiency factors detailed in equations 10, 11, and 12 [8, 11]. The molecular mass, M, again appears, but this time in the denominator. In this case, the lighter propellants, like krypton are the most mass efficient, meaning higher Isp. As discussed above, iodine may act as a heavier propellant. If this is the case, Isp will suffer. Heavy propellants like bismuth will have substantially lower Isp's than krypton. These lower Isp propellants will be less desirable for missions requiring rapid changes in velocity.

Table 1 shows a huge range of costs for the various propellants. Cesium is extremely high performing, but costs so much that it becomes impractical. Bismuth is a close second in performance while also being the second cheapest propellant. Particularly noteworthy is the cost of xenon. Xenon is still the most common propellant, but it is the second most expensive. Iodine is less than half the cost of xenon and is much more abundant. It is clear that cheaper alternatives exist, but testing is needed to prove usefulness.

Heating of propellants presents a whole new dimension to the Hall thruster problem. The propellants marked NA are already gases at room temperature, and will therefore require no additional heating. This is a clear advantage for xenon and krypton. The remaining propellants must be raised to the temperature at which sufficiency mass flow is vaporized. Some propellants must be closer to the boiling point than others

before the necessary mass flow can be achieved through vacuum vaporization. Also, specific heat will come into play when determining the power required to heat a propellant to its melting point. Latent heat of fusion will need to be overcome when melting the propellant because simply raising the temperature of a substance to the melting point does not transition its phase. Latent heat of sublimation similarly accounts for the direct transition from solid to gas. These values will differ greatly based on the specific properties of the substances.

One good point of comparison is to look at the melting points of the propellants, which are shown in Table 1. Several metals show some promise in the low melting points, like mercury for example. Mercury has a low enough melting point that no significant heat will have to be added to keep it a liquid on board a spacecraft. Cesium also has a relatively low melting point. Bismuth has a clear disadvantage in this area. Iodine has a low melting point, but does not have the lowest melting point. However, when boiling points are examined, the metals become less appealing. From this data set, vaporizing metals is more difficult than the non-metal propellant like iodine. Iodine has a conveniently narrow liquid phase vs. temperature. Bismuth in particular is quite difficult to vaporize making it less desirable.

Thrust-to-power ratios are important in measuring the usefulness of a Hall thruster. The calculation for thrust to power solely based on thruster performance is given by;

$$\frac{T}{P_T} = \frac{2\eta_T}{g \cdot Isp} \tag{5}$$

where η_T is an efficiency factor, and P_T is the power consumed by the thruster [8, 11]. This equation does not account for the power used to heat the propellant. This may be a

concern on a spacecraft with a limited power budget. A more accurate model for the thrust to propulsion subsystem power ratio would include this additional heating into this calculation. This adjustment would normalize the above data and help compare dissimilar propellants by including the heating loss.

The data suggests that iodine is a worthwhile propellant to investigate. The molecular mass means possible higher thrust numbers than xenon. Theoretical ionization shows that iodine has the potential to produce more efficiency. Cost can potentially be improved by switching from xenon. Melting and boiling points show condensed propellant could be vaporized more easily than the metal counterparts. Additionally, the storability of iodine is more convenient than xenon. Neglecting the mass of the tanks required to contain xenon, the propellants would have the same density if the xenon were stored at about 850 atmospheres. This is an extremely high pressure just to reach iodine standard storage conditions. The propellant looks good on paper. The next challenge is to design an experiment that will accurately measure the iodine operation.

II.4 Experimental Considerations

Experimentally, this is a difficult problem. Iodine propellant is in its infancy and therefore unforeseen problems are likely to arise. Inputs will need to be closely monitored to ensure proper operation. Since the propellant is condensed, this will now include temperature on top of the typical Hall thruster parameters.

Optimal parameters are unknown for iodine Hall thruster operation. There are little data to support the theoretical work. The input conditions need to be adjusted to ensure iodine operates properly. The iodine must also be operated at the same condition

as xenon. This allows for a more intuitive comparison of the two propellants. The thruster operation is only part of the experimental considerations. The diagnostic equipment is just as important to the success of the experiment. Both of these components must physically survive the experiment to give reasonable and repeatable results.

The biggest concern in this experiment is the corrosive nature of iodine. Intrusive probes will be put directly at risk for corrosion from the ionized iodine exhaust. A possible outcome is that not enough data is collected to truly understand the mechanisms involved in the iodine propellant problem because the probes cannot physically survive in the exhaust. Another concern is that the probes give faulty data based on the degradation of the measuring equipment. A possible solution is to test the probes for accuracy after using them for this experiment. Also, the iodine may corrode the thruster itself. The exhaust can erode the inside of the thruster more quickly than with a noble gas. Exhaust ions that were not properly neutralized may make their way back to the thruster and damage it. These damage mechanisms must be addressed before the experiment is executed. Once the equipment is found to survive the operation, the measurements can be made.

II.5 Performance Measurement and Plasma Diagnostics

In order to accurately gauge performance, the first step is to accurately know the input conditions. All the inputs to the equations will need to be known to a high degree of accuracy to get useful comparison data. Then, the measured values must be compared against experimental values. The values for comparison will include thrust, T. Thrust

can be measured by a sensitive inverted pendulum thrust stand. Specific impulse would be another value of interest. With the exhaust velocity of the thruster, it can be calculated.

$$Isp = \frac{u}{g} \tag{6}$$

Velocity measurements can be difficult. One available technique is to use laser-induced fluorescence. However, if thrust is measured and mass flow rate is known, exhaust velocity can be determined by equation 7 without a separate technique. Mass flow can be determined by a mass flow meter on the input flow line.

$$u = \frac{T}{\dot{m}} \tag{7}$$

Then, the equation for specific impulse becomes

$$Isp = \frac{T}{\dot{m}g} \tag{8}$$

Equally as interesting as finding actual thrust and specific impulse is to know the physical properties of the exhaust. This gives more insight into the mechanisms behind the final thrust and specific impulse numbers. It also details the losses in producing usable power to move a spacecraft.

One measuring device that can be used is the Langmuir probe. It provides a number of useful plasma properties for computing efficiencies in the Hall thruster. The main function of this probe is to find voltages in the plume. These voltages are useful in efficiency calculations. Another tool is the Faraday probe, which measures current density. It is a less intrusive probe, and provides current data in the plume. The current data produces separate efficiency numbers useful in determining overall efficiency. This probe is typically swept through the cross section of the thruster to provide good data for

the entire plume profile. Finally, a very useful probe is the ExB (pronounced E cross B) probe. It uses the Lorentz force to separate different ions in the exhaust. The probe gives good data on the efficiency of ionization happening in the Hall thruster. The ExB probe is also capable of producing similar data to the Langmuir probe without the separate instrumentation. The Langmuir, Faraday, and ExB probes each give separate information about the plume. These details give insight into the efficiencies of the thruster.

II.6 Efficiency Determinations

There are several measures of efficiency in Hall thruster. The collection of these efficiency factors gives the overall efficiency factors needed for calculating performance parameters. Below is a discussion of these efficiency factors and how they are found.

The overall efficiency of the Hall thruster is the product of all the smaller efficiency factors according to Kim and is given by:

$$\eta_T = \frac{I_i}{I_d}\eta_i\eta_\beta\eta_v\eta_\varepsilon \tag{9}$$

I_i represents the ion current, and I_d represents the discharge current [12]. The first efficiency, η_i, is the propellant utilization efficiency. It is represents the fraction of propellant used to produce usable thrust. η_β is the beam focusing efficiency which essentially is the correction factor needed for the divergence in the exhaust. The efficiency term η_v accounts for the different velocities of the exhaust ions. Lastly, η_ε describes the efficiency inherent in accelerating the ions from nearly stationary to their final velocity [12].

Separately, Goebel and Katz express total efficiency as;

$$\eta_T = \gamma^2\eta_b\eta_v\eta_m\eta_o \tag{10}$$

η_b is the beam current efficiency which relates the ion and discharge currents similarly to above but with beam current instead of ion as;

$$\eta_b = \frac{I_b}{I_d} \tag{11}$$

Along the same line, η_v represents the identical voltage ratio

$$\eta_v = \frac{V_b}{V_d} \tag{12}$$

η_m is a mass utilization efficiency term. It relates the mass flow from the anode and cathode, $\dot{m}_a$ and $\dot{m}_c$ respectively, to the mass flow of ions out of the thruster, $\dot{m}_i$. The cathode flow rate can be ignored in this equation to find anode efficiency rather than total thruster efficiency.

$$\eta_m = \frac{\dot{m}_i}{\dot{m}_a + \dot{m}_c} \tag{13}$$

Then, η_o, uses the discharge power of the thruster, P_d, keeper power, P_k, and magnet power, P_{mag}, to find electrical efficiency. This term is only used in the total efficiency calculation.

$$\eta_o = \frac{P_d}{P_d + P_k + P_{mag}} \tag{14}$$

The plume geometry is communicated in γ. It accounts for both plume divergence and multiple ionizations.

$$\gamma = \alpha F_t \tag{15}$$

α is based on the ionization characteristics. If I^{++} is the number of doubly ionized particles and I^{+} is the number of single ionized particles, then α is given by;

$$\alpha = \frac{1 + \frac{I^{++}}{\sqrt{2} I^{+}}}{1 + \frac{I^{++}}{I^{+}}} \tag{16}$$

When the equation is arranged in this fashion, the number of ions need not be known. The ExB probe is able to measure this ratio to calculate this factor. The potential exists to further expand this equation to possibly account for more ionization states. Iodine in particular is susceptible to more than two commonly occupied ionization states. Monatomic iodine has two common positive ionization states as well as one negative ionization state, while diatomic iodine has one common positive ionization state and one negative ionization state.

The F_t term accounts for the geometry of the exhaust plume. It uses the angle off thrust axis, θ, and the ion current density, j_b, to find geometric efficiency;

$$F_t = \frac{\pi R^2 \int_{-\pi/2}^{\pi/2} j(\theta) \sin(\theta) \cos(\theta) d\theta}{I_b} \tag{17}$$

The Faraday probe can experimentally determine the values of j_b at different values of θ.

In short, there are many terms to track in order to back out overall performance of a Hall thruster. Hall thruster operation depends on the properties of the propellant and thruster operation. According to the first order theory, iodine is higher thrusting and more efficient than xenon. Further investigation with thrust stand measurements and plume probes will confirm this. The plume probes are used to find the separate efficiencies that combine to give the total efficiency. Isolating these efficiencies reveals the details of the thruster operation for better comparison of iodine and xenon. The experimental data will show the usefulness of iodine as a propellant.

III. Methodology

The experimental method is the key to producing a sound argument. This chapter provides the details of the set up and the equipment. The experiment analyzed iodine operation in two ways. First, thrust and thruster operating condition determined the efficiency, specific impulse, and thrust to power ratio. The thruster operating condition data relevant to the data reduction were mass flow rate, discharge current, and discharge voltage. This data was referred to as the performance measurements. Then the plume diagnostics were used to determine the efficiency. The individual efficiencies were multiplied to give a total efficiency. This data was referred to as the plume measurements. Plume and performance measurements were compared in order to validate and identify possible sources of error for efficiency. This process was repeated for xenon operation to be used as a comparison. The equipment was consistent for all data sets to make better comparisons.

Figure 4 shows the basic setup of the entire experiment. The vacuum was maintained by the diffusion pump to the top. The thruster was opposite the pump. The thruster was fed through the vacuum boundary with the iodine and xenon reservoirs selectable through a three-way valve. The ExB probe was positioned downstream of the thruster, fixed in the plume. The Faraday probe was swept on an arm through the plume. The thrust stand supported the thruster just above the pivot of the sweep arm. All of the drawing systems were over simplified, but the general setup was shown. The thruster was the main piece of equipment used; it was required to handle all operating conditions.

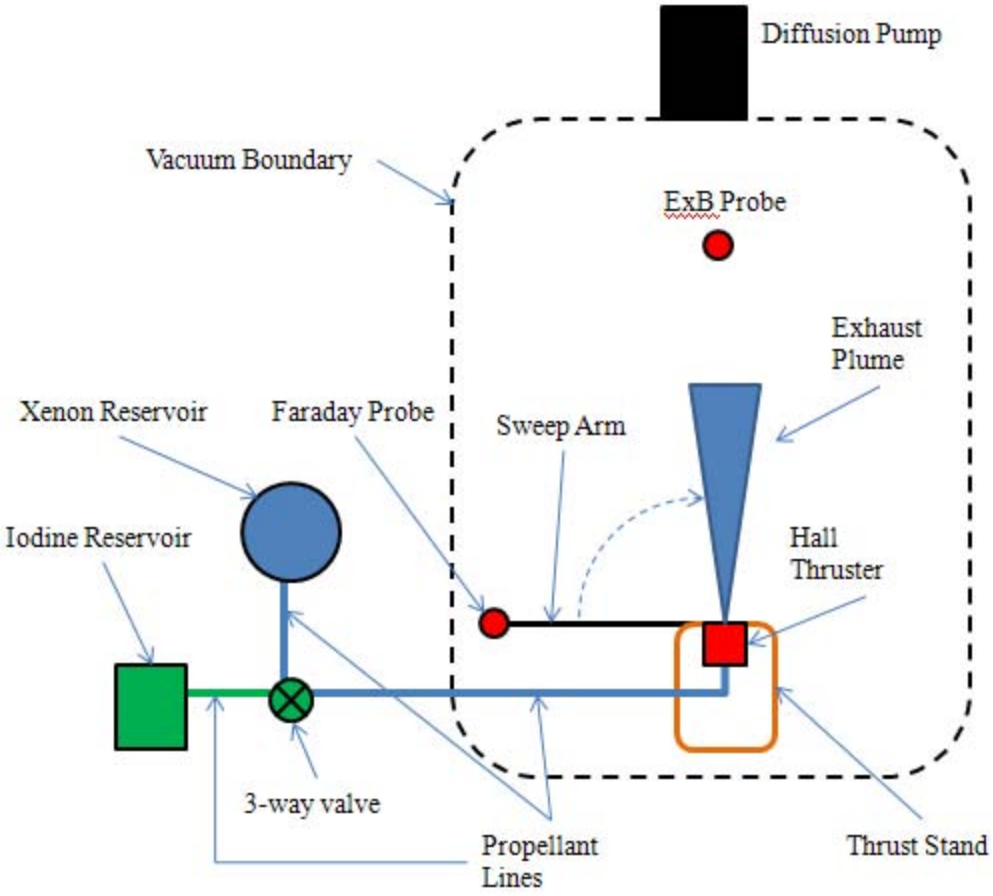

Figure 4: Overall experimental setup of the vacuum

III.1 Thruster

The BHT-200 thruster developed by Busek Co. was used in this experiment both for the iodine and xenon operation. The BHT-200 is a well known, highly characterized thruster proven in space missions. It was used with a BHC-1500 hollow cathode mounted in standard configuration as shown in Figure 5 and Figure 6. The BHT-200 is a 200 Watt hall thruster. The xenon nominal operating condition is 250 volts and 800 milliamps discharge. This condition was chosen as a baseline for iodine testing. The thruster and cathode were powered by a Busek developed power processing unit (PPU)

designated the BPU-600. The PPU was powered by a 30 volt, 30 amp power supply. Components were monitored and controlled through a LabView interface.

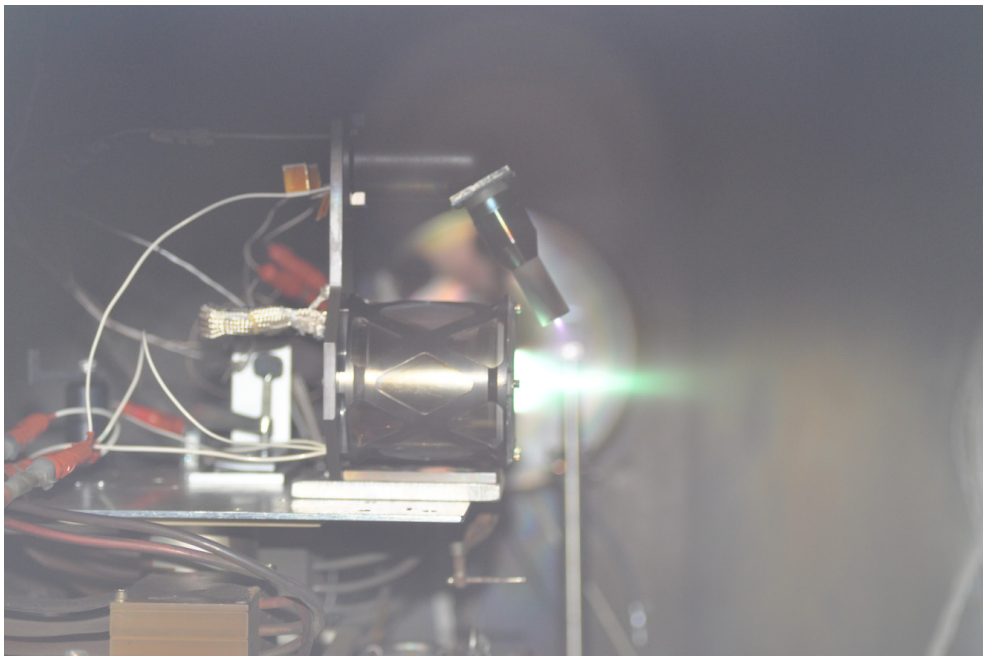

Figure 5: BHT-200 and BHC-1500, side view

Figure 5 shows the BHT-200 operating with iodine. The cathode was mounted in standard configuration above the thruster. The thruster is operating in jet mode, meaning the plume is highly directional. The Faraday probe sweep arm is visible in the background of the figure. Directly behind the thruster, the heated feed line to the anode is visible as a pale, braided feed line.

Figure 6 is similar to Figure 5. The BHT-200 is shown from the front in this view. The thruster is mounted on the thrust stand, ready for operation. In this figure, the thruster is connected but not on.

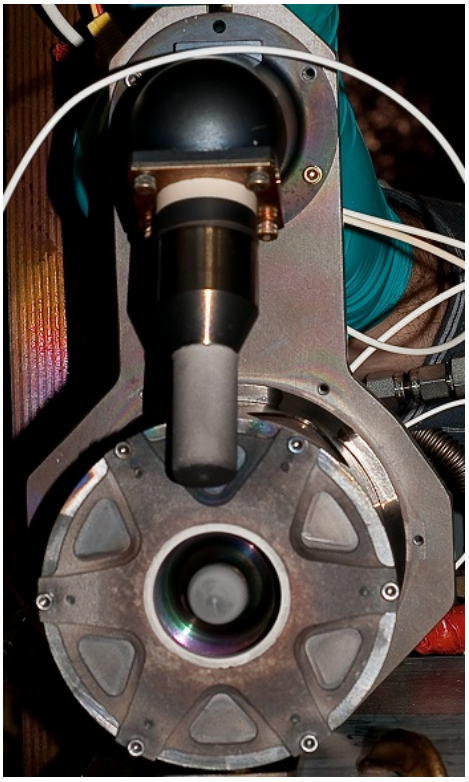

Figure 6: Busek BHT-200 and BHC-1500, front view

III.2 Testing Facility

The thruster was placed in the T6 vacuum facility at Busek Co. The tank is 1.8 meters in diameter. It is connected to an 81 centimeter diameter diffusion pump used to evacuate the gases at low pressure at a rate of 17,000 liters per second. A mechanical roughing pump is used to bring the tank to a suitable pressure for diffusion pump operation. The chamber is also fitted with cryo-pumps which were not used in this experiment. Tank pressure was monitored with a Bayard BPG400/VCG401 gauge. Pressures during thruster operation were as low as 6 x 10^{-6} torr on iodine and 2 x 10^{-5} torr on xenon.

Figure 7: Busek T6 vacuum facility

Figure 7 shows the side view of the vacuum chamber used in the experiment. The diffusion pump was located to the far left of the figure, behind at the rear of the chamber. The thruster was located inside the chamber on the far right as shown in the figure and facing to the left. The feed system is not pictured, but was located on the side of the chamber, behind the blue equipment tower pictured.

III.3 Feed Systems

The xenon flow was regulated by Unit 7300 flow controllers from Unit Instruments. A 50 SCCM controller was used for the anode flow, while a 10 SCCM controller was used for the cathode flow.

Highly pure iodine was stored in a heated reservoir outside of the chamber. The iodine was sublimated by varying temperature in the reservoir. The iodine then flowed through a series of heated stainless steel and Teflon tubing to the thruster anode. Flow line temperatures were heated to at least 60 degrees Fahrenheit above the reservoir temperature to ensure no deposition occurred before the iodine is discharged. Omega CN4000 PID temperature controllers were used to regulate all temperatures. Absolute pressure was monitored upstream of the anode flow line. Mass flow rates were then correlated to this pressure.

III.4 Diagnostic Equipment

The instrument used to take thrust measurements was the Busek T8 inverted pendulum thrust stand [13]. The stand houses a linear variable differential transformer (LVDT) which converts linear displacement of the stand pedestal to a voltage. The pedestal was connected to the base by eight flexures. The flexures are replaceable and have varied stiffness. The stiffness was chosen to keep the LVDT in the linear range for the amount of thrust expected. A spring was used to create additional damping and center the pedestal. The thruster was mounted directly on top of the pedestal.

Figure 8 shows the thrust stand with the thermal jacket removed. The horizontal plate to the far right is the main moving piece of the assembly. The pedestal rests over the black cylinders. The LVDT is attached to the left side of the horizontal plate. Below the plate are the two flexures described above.

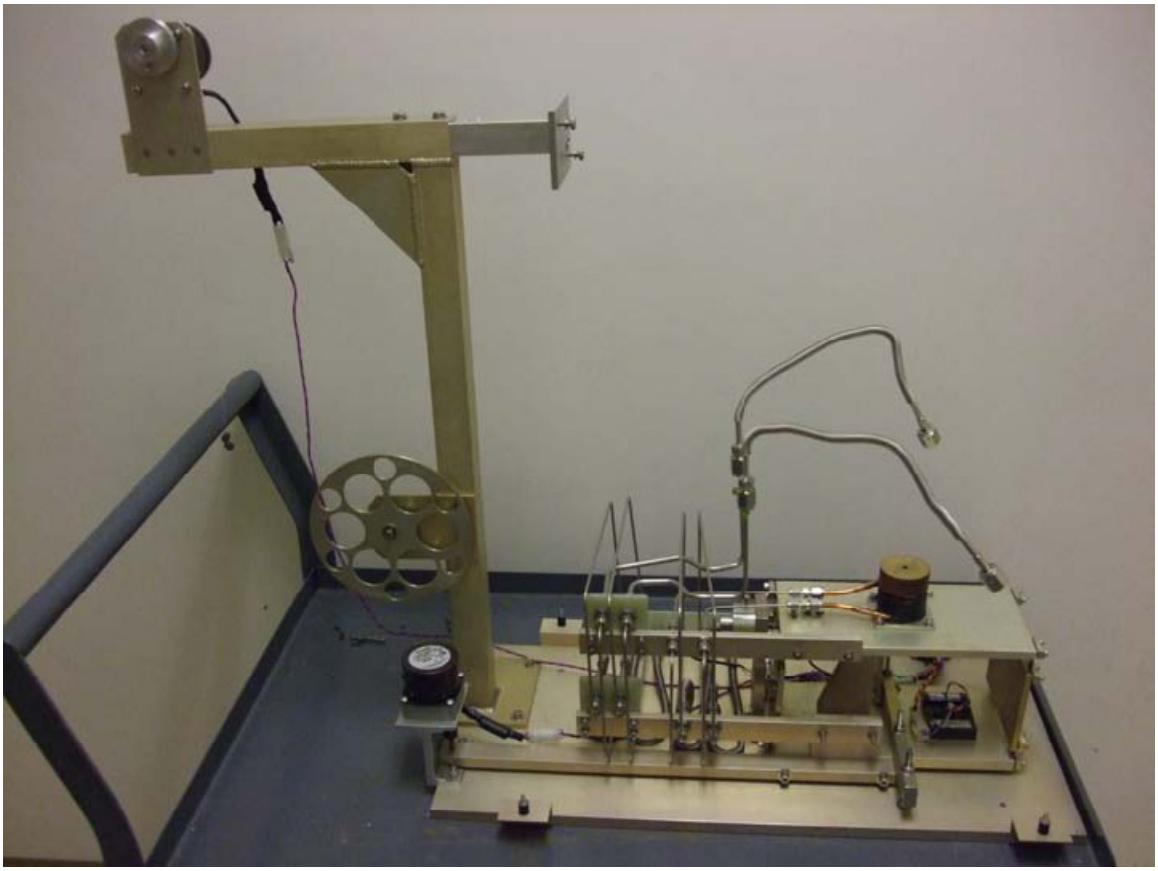

Figure 8: Thrust stand with cover removed, taken from Temkin [14]

Surrounding the movable components was a thermal jacket to maintain temperature. It functioned by isolating the components from the plasma in the thruster plume and creating a uniform temperature surrounding the sensitive LVDT. The LVDT was then assumed not to thermally drift during thruster operation.

Figure 9 shows the thrust stand fully assembled. The thermal jacket is covering the inner electronics of the thrust stand. The silver pedestal is protruding from the thermal jacket, which holds the thruster. The cooling lines are shown snaking along the thermal jacket, designed to keep the jacket at the desired temperature.

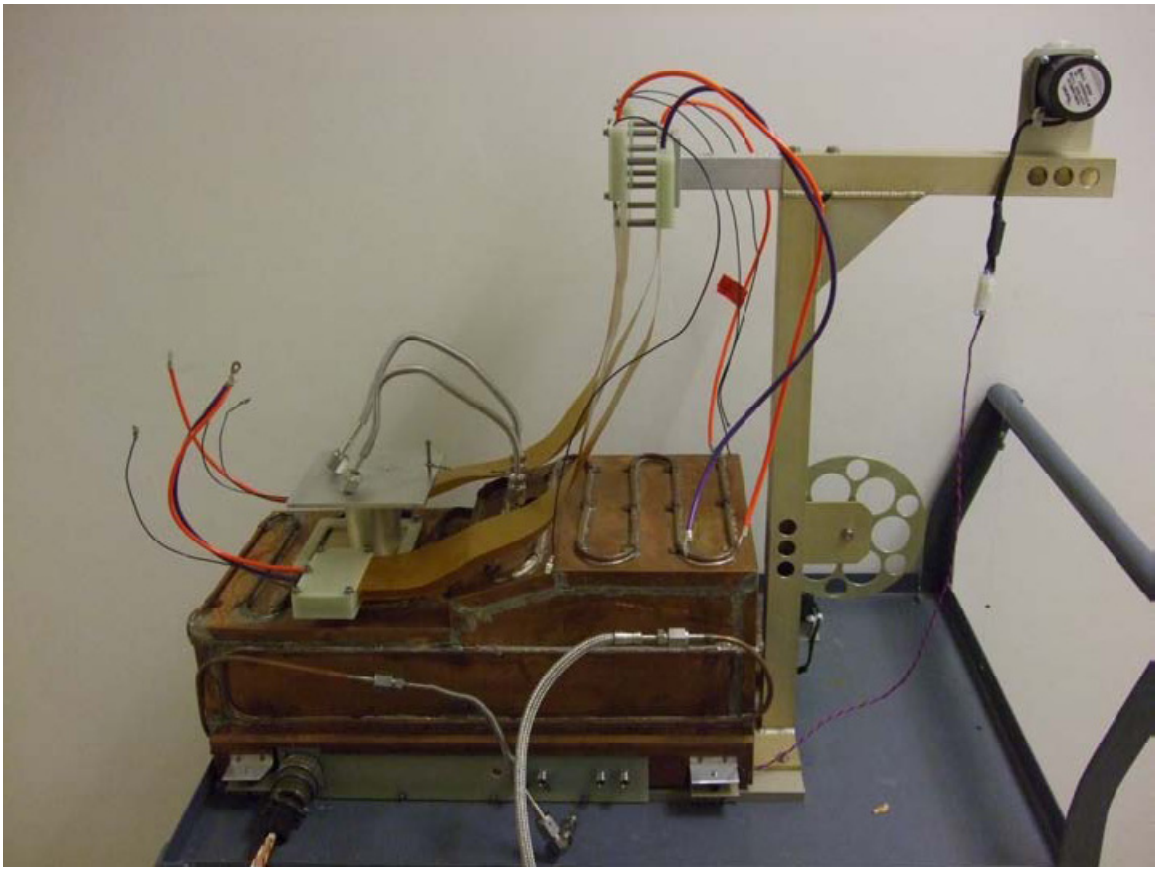

Figure 9: Thrust stand with thermal jacket and wiring installed, taken from Temkin [14]

In order to calibrate the system, a series of weights were hung from a pulley system on the thrust stand. The weights were approximately 0.42 grams each. Each weight was loaded and unloaded by a motor attached to the stand. The motor was controlled by a switch outside of the tank. A Labview interface recorded amplified outputs from the LVDT and generated time averages of the readings. From this data a response function was generated to determine thrust from LVDT voltage. Thrust was taken at each thruster operating condition once discharge current was given ample time to settle. Prior to each change in thruster operating condition, a new zero thrust voltage for the LVDT was taken to ensure any drift would not have time to accumulate. Time

averages of thrust were taken for approximately one minute, although average values did not typically change after 10 seconds.

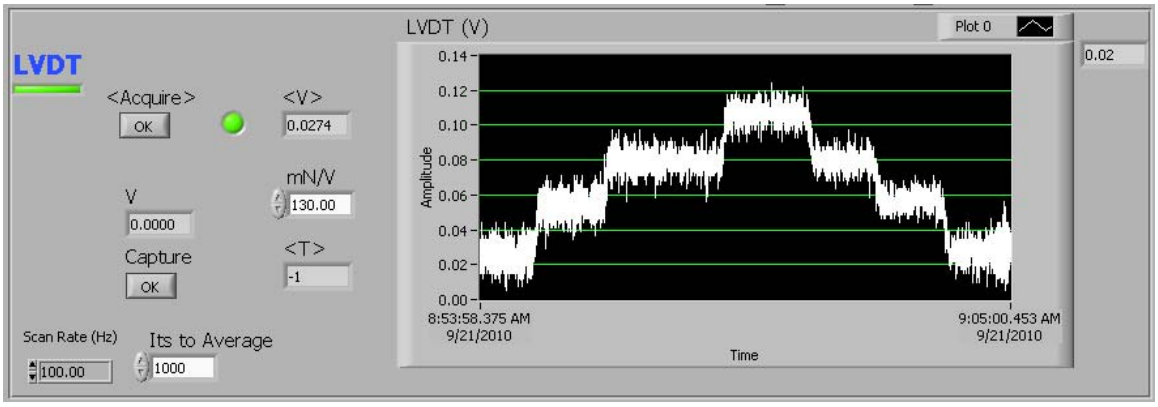

Figure 10: LVDT LabView interface

Figure 10 shows the LVDT output to LabView after adding and removing the calibration weights. The noise is significant in the voltage readout, but the averages are very stable. The zero calibration weight voltage is visibly the same before and after adding the weights. The measurements are taken at a rate of 100 Hertz as shown in the lower left hand corner of the output. The slope of the calibration curve is adjusted in this program to estimate thrust. This program also time averages the data automatically and outputs the average voltage over the time span.

The thrust stand was mounted in the vacuum chamber as shown in Figure 11. The entire assembly was mounted semi-permanently in the chamber on 80/20 aluminum. The structure was leveled before the thrust stand and thruster were placed in the chamber. The thruster was leveled and centered in the chamber directly over the Faraday probe sweep arm. Thrust was not the only measurement dependent on the proper alignment and leveling of the equipment. The Faraday probe data depended greatly on the success of the setup of the thruster.

Figure 11: Thrust stand mounted in the Busek T6 vacuum tank

A nude Faraday probe was the main instrument used in the plume diagnostics. Faraday probes are straight forward instruments used to extract beam current from the plume. This probe was originally developed at MIT [15]. This probe was cross-calibrated against a larger and well-characterized JPL probe [16]. The probe consisted of a collector plate which was directly exposed to the plume. Around the collector plate is a guard ring which is biased negatively to 20 volts to repel electrons. The function of the ring is to ensure low energy ions from the sides of the probe do not contact the collector plate. The collector plate is biased to the same voltage as the guard ring. This was done to repel electrons and ensure a uniform potential field. This potential field creates a sheath discouraging low energy ions from entering off axis. Figure 12 shows the Faraday probe detector with no cover installed. The center flat plate is the detector plate, and the casing around the edge is the guard ring.

Figure 12: Nude Faraday probe with casing removed, taken from Azziz et al. [17]

When the bias is properly applied, only ions moving directly towards the collector plate will induce a current. The current induced depends on the ion current flow, which is the desired parameter, the material used for collection, and the species in the plume. Under ideal conditions, an ion would collide with detector plate causing neutralization of the ion. The electrons supplied by the collector plate to neutralize are replenished through the probe circuit. This would result in an ion current equal to current in the circuit. However, each material and ion pair will have a unique probability of secondary electron emission, called the secondary emission yield. A secondary electron emission occurs when an ion collides with the detector plate and the plate emits an electron not involved in the neutralization. This causes higher measurements than expected. Typical detector materials have known secondary emission yields when influenced by xenon ions. Secondary emission yields for iodine, on the other hand, are not well known. The material used for the collector was 316 stainless steel sprayed with tungsten for reduced secondary emissions. Previous research conducted with this probe assumed no secondary emissions [17]. The data reduction in this research made the same assumption.

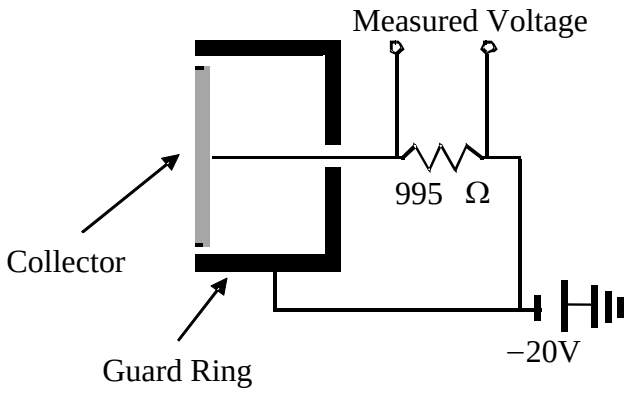

Figure 13: Faraday probe wiring diagram

The current density was not directly measured. Voltage across a resistor in the probe circuit was measured at each data point. The resistance and the collector plate were used to find the desired parameter, current density, as in equation 18. Figure 13 illustrates the wiring setup of the Faraday probe. The collector on the left side is the same component as in the front of Figure 13. The voltage measured across the resistor was acquired and read through LabView software interface.

$$j_b = \frac{V}{R \cdot A_{aperture}} \tag{18}$$

Then, with the current density, current in the plume could be estimated. Equation 19 was used to calculate current by assuming all of the current was moving towards the back of the tank. Additionally, the plume was assumed to have radial symmetry on the left and right side of the thruster. This assumption created a half-spherical shell of known current densities.

$$I_b = \pi R^2 \int_{-\pi/2}^{\pi/2} j(\theta) \sin(\theta)\, d\theta \tag{19}$$

The integral was evaluated numerically using a trapezoidal method. This was slightly more accurate than methods used previously.

An ExB probe was also used to examine the plume. This instrument filtered ions passing into the probe by their velocities. The ExB probe used in this experiment consisted of four sections. The first was the collimator. The collimator was grounded unlike the Faraday probe entrance because the detector was not up front as before. The aperture was small, 0.381 millimeters in diameter, to minimize the acceptance angle of the probe, which is within $\pm$0.3 degrees. The length in the collimator also contributed to the acceptance angle.

The next stage was the ExB stage where the actual filtering was accomplished. The particles entering this section were subject to the Lorentz force.

$$\vec{F} = qe\left(\vec{E} + \vec{u} \times \vec{B}\right) \tag{20}$$

Those particles that had no net force on them passed straight through this section. The probe was built such that the electric field, magnetic field, and ion velocities were all perpendicular to one another. The equation for ion velocity was found by setting force equal to zero along with the perpendicular assumption.

$$u = -\frac{E}{B} \tag{21}$$

The magnetic field came from internal permanent magnets. The electric field was adjusted by changing the potential between a known gap with a Keithley 6487 picoammeter and voltage source. Negative potentials were used based on the solution of equation 21. The electric field strength was known from the applied potential, ϕ, and the gap size, d.

$$E = \frac{\phi}{d} \tag{22}$$

This means that the velocity of the particles passing through this section of the probe is known for each potential.

$$u = \frac{\phi}{Bd} \tag{23}$$

The velocity of ions leaving the thruster is given by Goebel and Katz [8]

$$u = \sqrt{\frac{2qeV_d}{M}} \tag{24}$$

This means that the discharge voltage can be solved for based on the conditions of the ExB and the ion species [18].

$$V_d = \frac{M}{2qe}\left(\frac{\phi}{Bd}\right)^2 \tag{25}$$

The discharge voltage was not the discharge voltage output from the PPU, but rather what the ion felt as it was accelerated out of the thruster. The voltages should were all lower than the PPU discharge voltage. Voltage efficiency was calculated using these values.

The next section was a simple drift region. This ensured that ions which were significantly perturbed by the ExB section yet made it to the back of the section did not make it to the collector. Only the ions still moving axially will arrive at the detector. The drift region was grounded like the collimator.

The last section was the detector region. The detector was similar to the Faraday probe detector, but made of tungsten rather than stainless steel. It was biased to -30 volts to discourage the electrons, like the Faraday probe detector. Also like the Faraday probe detector, secondary emissions were ignored in data reduction. This provided conservative numbers for efficiencies, since doubly and triply charged species were more

likely to produce secondary emissions. Correcting for this effect revealed less of these species, resulting in higher efficiencies.

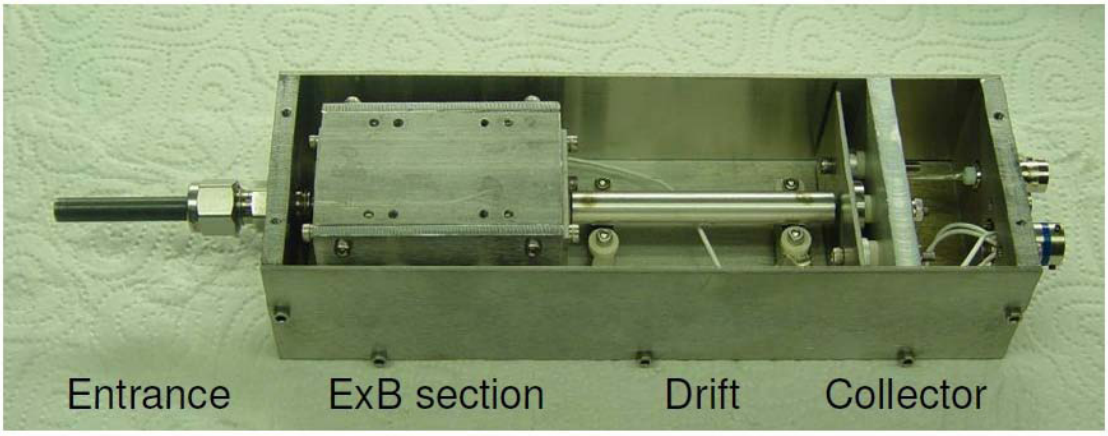

Figure 14: ExB probe with cover removed, taken from Farnell and Williams [19]

The ExB probe is shown in Figure 14 with the cover removed. Each of the regions discussed above are labeled separately. The ions enter axially from the left and are detected on the far right plate. The inputs and outputs are measured from the far right two ports.

The ExB circuit had three inputs, one output, and a ground. The ground was common to the input cannon plug cable and the BNC output. Two of the inputs were used to bias the plates creating the electric field. The other input was used to bias the collector plate. The BNC output was measured by the same Keithley 6487 picoammeter and voltage source used to create the plate potential.

The ExB circuit is illustrated in Figure 15. The sweep voltage is shown in the center bottom directly changing the potential between the plates of the ExB section. The ground is applied to both the collimator and the drift regions, but this is not shown. The suppressor is shown on the far right, biasing the collector plate to reject electrons.

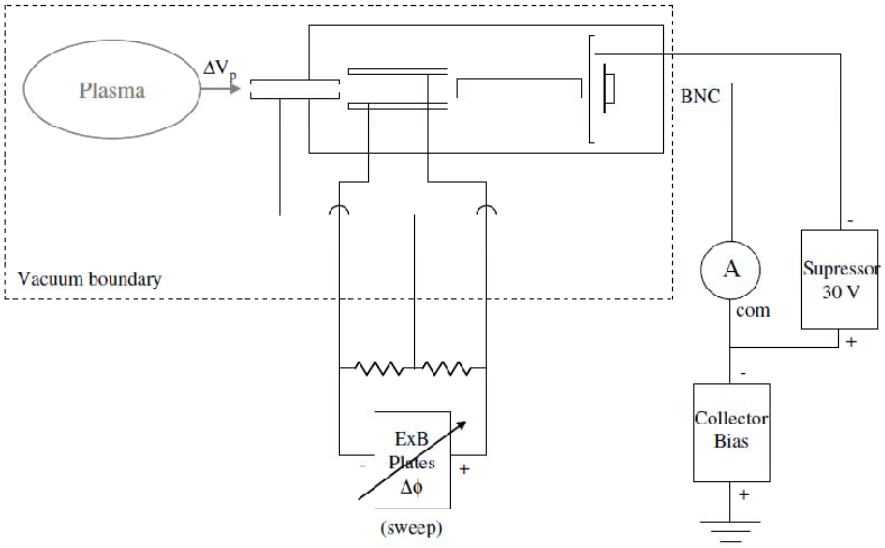

Figure 15: ExB probe wiring diagram, taken from Farnell and Williams [19]

The diagnostic equipment used in this experiment was selected to gain the most insight into the performance of the thruster. It was essential to understand the how these instruments operate in order to gain useful information from them. It was important to set them up properly. However, a properly used instrument is not the only variable in getting useful data. The application of these instruments was just as important.

III.5 Experimental Setup

Identifying the methods for using the diagnostic equipment and the processes for using the equipment was critical to the success of the experiment. The Faraday and ExB probes must be operated efficiently to save time and decrease time dependant factors.

The Faraday probe was mounted on top of a fixed radius automated rotating arm. The radius was 60.2 centimeters from the face of the thruster. The arm was swept 90 degrees from the thrust axis in both directions, bisecting the plume. The thruster centerline was laser leveled to be in plane with the arm sweep radius. The arm was swept in one degree increments with a dwell time of five seconds per angle. At the end of the

dwell, several measurements were taken, and a single average was calculated in the LabView software and output to a data file.

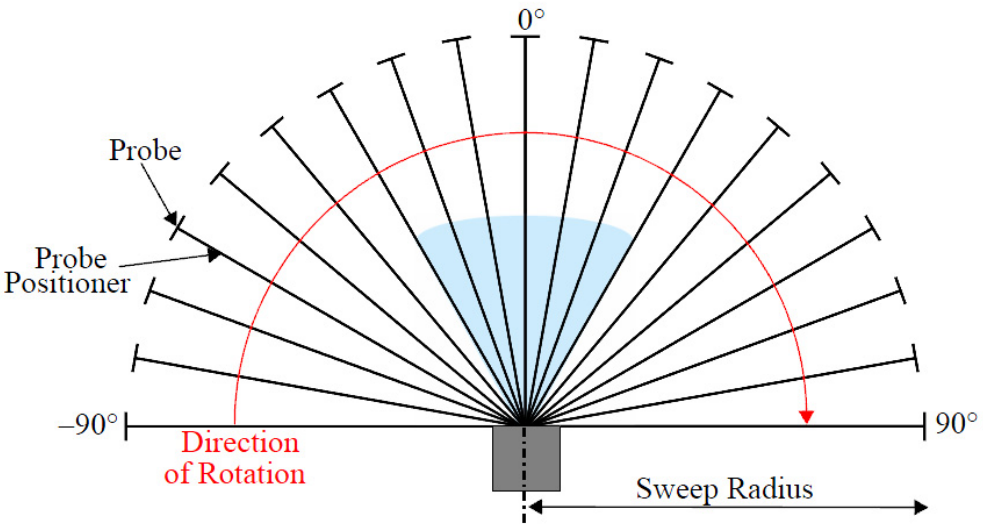

Figure 16: Faraday probe sweep profile, top view, taken from Azziz [15]

Figure 16 shows the sweep pattern of the Faraday probe. The thruster was positioned directly above the pivot point of the sweep arm. The arm moved 180 degrees from one side of the face to the other from the left to the right. The radius and height were constant throughout the sweep. Although the Faraday probe requires at least two dimensions of data to give useful data, the ExB probe is be useful at a single position.

The ExB probe was mounted on a stationary stand constructed from 80/20 aluminum. The probe entrance was positioned 108 centimeters from the face of the probe. The aperture was aligned via laser level with the center axis of the thruster. The voltages were chosen such that triple ionizations could be observed for both iodine and xenon. For a typical nominal condition, 250 volts discharge, 35 volts for the electric field potential was sufficiently high to capture all of the observable species. A LabView

program interfaced with the picoammeter. The program automatically swept from zero volts to the desired maximum in 0.1 volt increments. The software took 100 measurements per voltage level and output them to a data file.

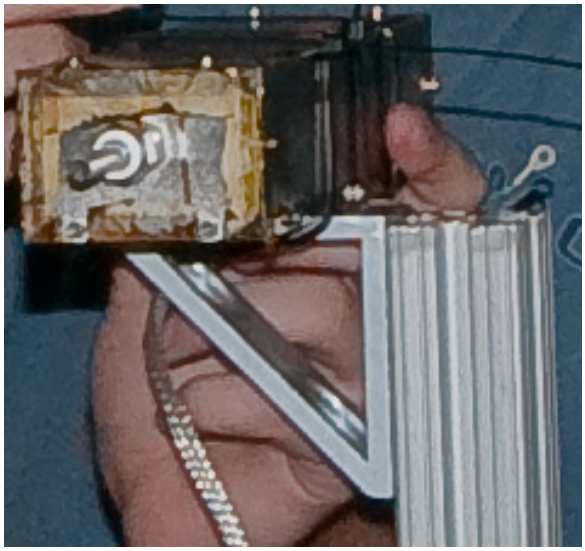

Figure 17: ExB probe mounted in front of the thruster

Figure 17 shows the ExB probe being mounted on the 80/20 aluminum. The braided wiring below the probe was the shielded input cable to the probe. The BNC was also shielded, but is not shown here. The probe was wrapped in Kapton tape to prevent extraneous ions from entering the probe through small openings. Separate from the probe conditions was the thruster conditions.

III.6 Operating Conditions

Chapter 2 showed how the thruster operating conditions must be known to make useful observations and comparisons. As discussed, the xenon nominal condition is 250 volts and 800 milliamps discharge. This is a useful condition to compare against xenon, since it is widely studied. Thruster limitations bounded the operating condition space. The thruster has a lower bound for both discharge voltage and discharge current due to

stability. At about 100 volts, the thruster has some trouble sustaining a steady operation. Thrust instability drove the lower bound to be 150 volts, in order to be certain of normal thruster operation. The high end of voltage is not well understood this early in research. Chapter four discusses this in more detail. However, experience with the thruster on iodine yielded confidence up to at least 300 volts. Although the thruster was successfully operated at higher voltages, 300 volts was the maximum in this experiment because of the sustained operation required for the test. Similarly, discharge currents above one amp were not tested. Low discharge currents cause some instabilities in the thruster as well. The magnet tends to pinch off the flow and drive the thruster into high current mode. Therefore, 500 milliamps was the baseline minimum for current.

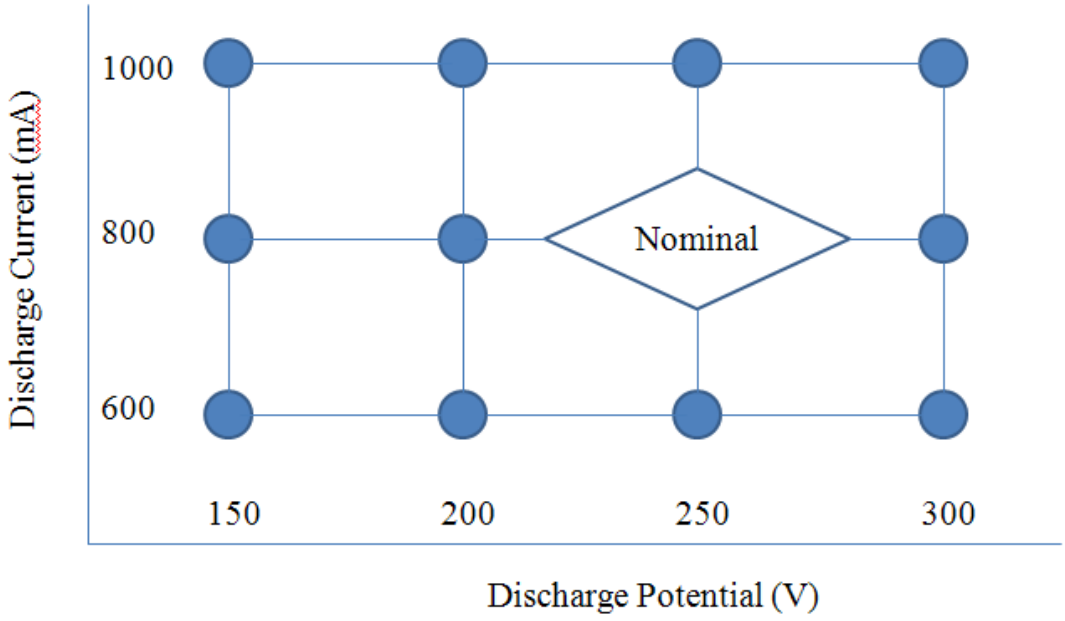

Figure 18: Thruster operating condition test-space for discharge potential and current

Figure 18 illustrates the approximate test conditions run for both xenon and iodine. Each of the blue dots represented a test condition for the propellant. To

adequately cover the solution space, 50 volt increments were chosen to give four possible discharge voltages, each of which had a minimum of three discharge currents. The discharge potentials ranged from 150 volts to 300 volts. The discharge current numbers were more like guidelines than actual test points, since the current is not directly controlled. Thrust and Faraday probe measurements were taken at each of the test points. Due to time constraints, only 250 volts discharge was examined with the ExB probe.

III.7 Uncertainties

Several sources of uncertainty were identified in the experiment. For the thrust stand, four sources of uncertainty were quantified. The first source came from the initial calibration of the stand. Each data point in the calibration was not measured exactly as the one before. From the curve fit data, a calibration uncertainty, e_{cal}, was calculated in equation 26 to account for this difference in measurement. N was the number of data points, y_i was the measurement, and $\bar{y}_i$ was the calibration value.

$$e_{cal} = \sqrt{\frac{\sum(y_i - \bar{y}_i)^2}{N}} \tag{26}$$

As discussed in the diagnostic equipment section, the thrust stand does had some drift during operation. This was quantified as a drift uncertainty, e_{drift}. The drift uncertainty was calculated using the new "zero" thrust after each run, ${T_0}^-$, and comparing it to the thrust before that run, ${T_0}^+$. The difference was averaged for all runs.

$$e_{drift} = \frac{\sum\left|\frac{{T_0}^+ - {T_0}^-}{2}\right|}{N} \tag{27}$$

The standard uncertainty of the equipment was also considered. The standard uncertainty was calculated by taken several measurements at the same condition and finding the standard deviation of that data set.

$$SE = t\frac{\sigma}{\sqrt{N}} \tag{28}$$

The final source of uncertainty was from the resolution of the instrument, e_{res}. This represented the amount of thrust variation that cannot be distinguished by the instrumentation. The total uncertainty was calculated from equation 18 [14].

$$\text{uncertainty} = \sqrt{SE^2 + {e_{drift}}^2 + {e_{cal}}^2 + {e_{res}}^2} \tag{29}$$

The total uncertainty in the thrust data was 0.224 milli-Newtons. This translated to about 1.5% of maximum thrust and 3.6% of minimum thrust measured.

Unlike the thrust uncertainty analysis, the uncertainty analysis for the Faraday probe was considerably simpler. The probe was swept through the plume of a thruster operating at a constant condition five times. The normal calculations were done including the current integration. These currents were normalized by the PPU discharge current. The standard deviation of these points was taken to be the uncertainty of the instrument. This uncertainty was calculated to be 1.9%.

The ExB probe analysis was done similarly, but there really are two separate total uncertainties in the instrument. The measured current at the detector is one uncertainty that is quantified. This correlates to the ion concentrations in the plume. The uncertainty is found by taking the several measurements at the same condition. The total current detected is counted. Then the standard deviation is taken for these totals and normalized by the average of them. The uncertainty in measured current is about 3.7% at nominal

xenon discharge current. The second uncertainty is the uncertainty in electric field potential, which correlates to velocity of the ions. This was calculated in the same way, by taking the standard deviation of the voltages at each peak at the same operating condition and normalizing by the mean. This uncertainty was calculated to be about 2.2%.

Overall, the experimental setup and data reduction was successful. The equipment used in the experiment was intended to find all of the performance characteristics and plume characteristics necessary to find efficiency; then, the data could be compared with xenon. This was accomplished with minimal error in a timely and efficient manner.

IV. Discussion and Results

This chapter addresses the findings of the experiment. Performance data is presented based on the thrust data and thruster operating conditions. Plume data is shown for each of the intermediate efficiencies. The plume efficiencies are compared with those from the performance data. Iodine is compared with xenon as a propellant from a performance standpoint. The heating of iodine is discussed as an efficiency loss for better comparison to xenon. Component degradation from iodine operation is discussed and suggestions to overcome them are made.

IV.1 Thruster Operation

Xenon propellant tests were successful. Operation was typical for this type of thruster. However, once the thruster had used iodine previously, the xenon operation changed somewhat. When the thruster was first turned on for the day, three distinct modes could be observed. First was the high current mode, which is characteristic of a thruster with the magnet turned off. This was seen when the voltage was high enough to create plasma in the plume. The current was physically limited to just above three amps. This mode was not desirable as significant thrust was not observed in this mode. The next mode was the minimum current mode. This was the preferred operation mode. Discharge currents appeared to be nominal in low current mode, and performance was roughly the same as historical data. Finally, there was a middle current mode. Typically, in this mode the discharge current was about 200 milliamps higher than in the low current mode. The thruster was significantly brighter from all observable angles in middle current mode. At first, it was hypothesized that residual iodine from the previous day

built up in the thruster, was heated by the xenon operated thruster, and was discharged along with the xenon. If this was the case, the xenon would operate in a constant condition. The residual iodine would slowly decrease as the iodine was sublimated and discharged. The observed operation did not support this conclusion. In actuality, the transition occurred suddenly and happened multiple times before low current mode was stable. Once the thruster transitioned to low current mode permanently, data was taken.

Despite the strange operation modes, iodine was successfully tested with BHT-200 thruster. Once the proper temperatures were achieved throughout the feed system, iodine flowed through the thruster with ease. The thruster was not directly heated, so the xenon was used to heat it up by running it at the nominal 200 Watt condition. The propellant feed lines were then heated to the operating condition of 150 degrees Celsius starting at the thruster and moving up stream. The partial pressure curve and mass flow calibration was used to determine the approximate temperature of the iodine reservoir. Experience helped finely tune the temperature for the desired operating condition. Temperatures around 80 degrees Celsius were selected for all operating conditions. Typically, the reservoir temperature was raised to 70 degrees and increased in one to two degree increments over several minutes until the desired pressure in the feed line was reached. Significant deposition occurred when the propellant lines were not heated significantly more than the reservoir or not heated properly. Additionally, iodine current did not settle once an operating temperature was reached. It took about 15 minutes to reach a stable condition. When the condition was adjusted, the iodine would increase slightly in discharge current, and then decrease over several minutes. This increased

uncertainty in measurements taken in short intervals and accounts for some of the uncertainty in mass flow rate.

The thruster started up once the iodine was heated and allowed to flow. The plume had a darker green plume, rather than the light blue plume characteristic of xenon. The two became more difficult to distinguish visually at higher power levels. Both plumes looked well formed and in jet plume mode for most conditions.

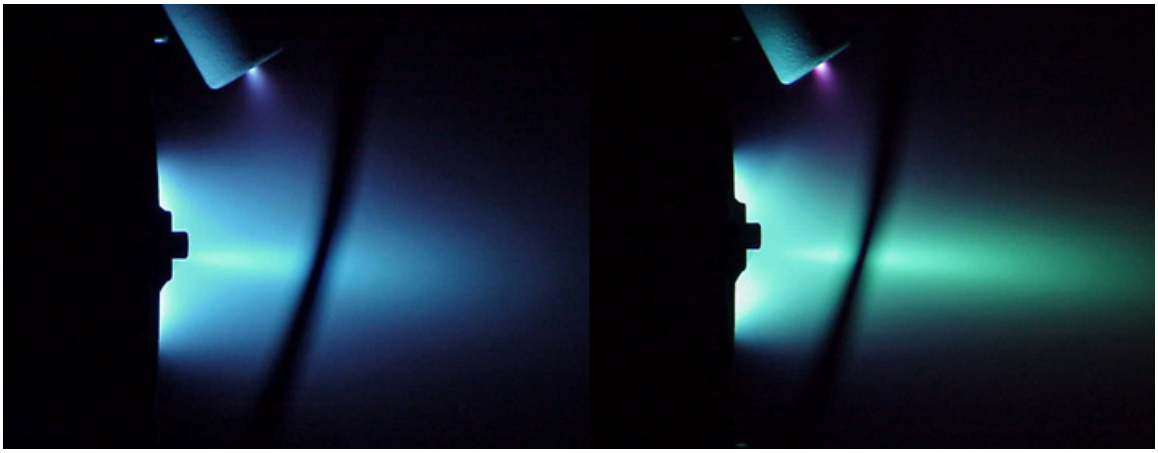

Figure 19: BHT-200 operating on xenon (left) and iodine (right)

Figure 19 compares the xenon and iodine operated hall thruster. Both of the propellants are running at the 200 Watt, nominal condition. Both propellants are operating in the jet plume mode which is observed in the thin bright lines along the thrust axis. The iodine is significantly more directional than the xenon. The xenon appears to spread out more quickly to the far off axis angles. This leads to efficiency losses discussed later in the chapter.

The BHT-200 had an optimal magnet current at which discharge current was minimized. The observed minimum was at 1.75 amps for xenon. It was important to keep comparisons as direct as possible, or they would be invalid. As a result, the magnet

current was set to the same current for both xenon and iodine operation. The operating conditions would probably be more optimal for iodine if the magnet current was altered, but then power consumption of the thruster would not be equivalent. The author chose to make direct comparisons rather than maximize the iodine performance.

IV.2 Performance Results

Thrust numbers were gathered with very little drift in the instrument. The drift was tracked between each run. As shown in Figure 20 and Figure 21, drift over an 8 hour period was roughly one milli-Newton, about 8% of nominal thrust.

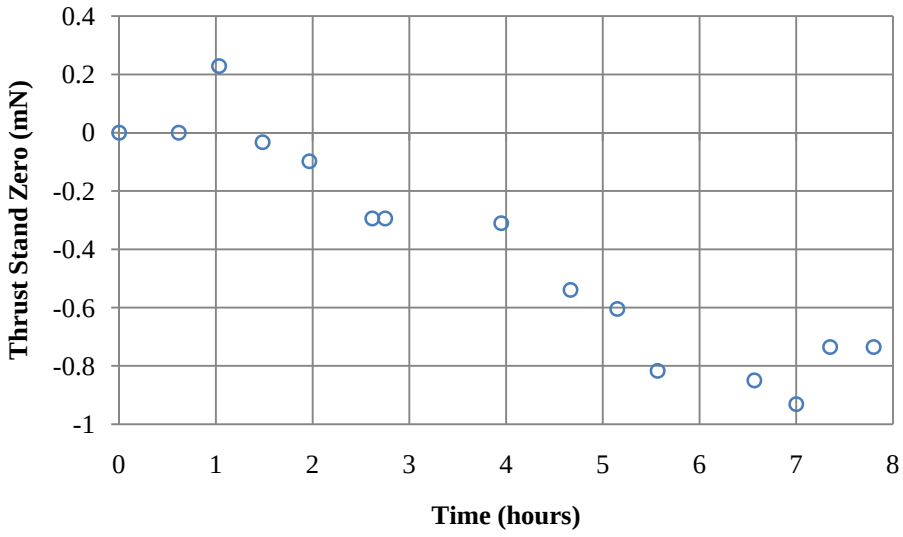

Figure 20: Thrust stand zero drift, day 1

Figure 20 shows each zero measurement taken on the first day of testing against the time from first run. The figure shows a predictable drift pattern with some minor fluctuations. The zero decreases with time at an approximate rate of 0.1 milli-Newtons per hour. The information effecting error is the difference in zero between each time

step. The maximum difference is only about 0.2 milli-Newtons. The frequent zero checks allow for a more confident analysis and smaller error.

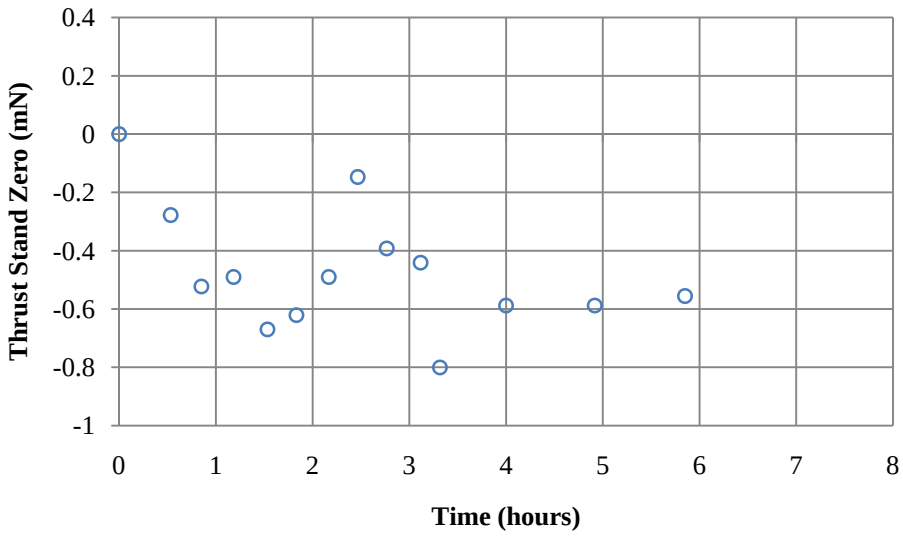

Figure 21: Thrust stand zero drift, day 2

Figure 21 also plots the zero thrust measurement, but on the second day of testing. The data in Figure 21 is similar to Figure 20 with subtle differences. The fluctuations are more severe, but trend in the same was as before. The range of fluctuations is decreased. This is expected since the second day of testing was two hours shorter. With the zeros closely monitored, accurate thrust measurements could be made.

Xenon thrust numbers were very close to previously reported numbers for this thruster [14]. Thrust numbers ranged from about 7.25 milli-Newtons at 100 watts to about 14.25 milli-Newtons at 300 watts. The iodine thrust numbers were more highly ranged than the xenon thrust numbers, ranging from about 6.75 milli-Newtons at 100 watts to about 15 milli-Newtons at 280 watts.

Figure 22 is a graph of the thrust data taken in the experiment. The thrust is normalized by discharge power so that all of the data can be incorporated into one curve.

The newly calculated thrust-to-weight ratio is plotted against discharge voltage. Generally, propellant thrust-to-power drops off with increased discharge current, and this is no exception.

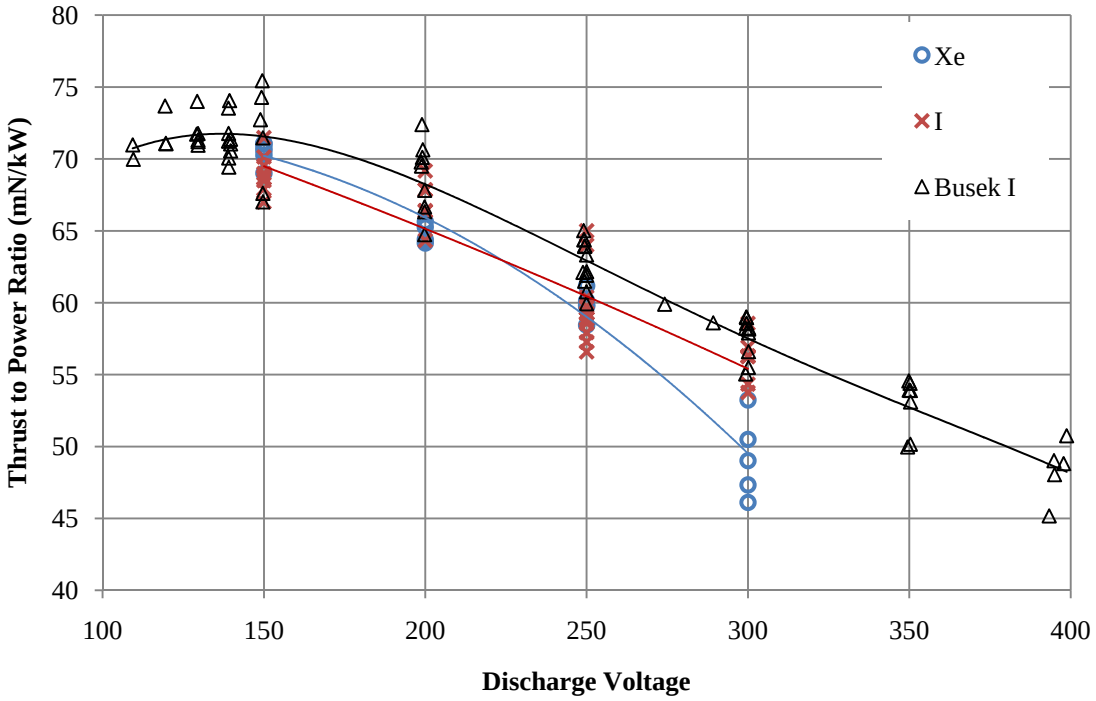

Figure 22: Xenon and iodine thrust to power ratio compared with Busek data

Xenon and iodine looked very similar from 150 volts to 250 volts. Interestingly, iodine outperformed xenon at 300 volts. Even the lowest iodine thrust to power was higher than the highest thrust to power for xenon. The average was a 12% increase in thrust on average at 300 volts. Thrust to power data for both propellants had similar variance. This was expected since thrust, discharge current, and discharge voltage were measured in the same way for xenon and iodine. Even more interesting than the superior iodine performance at 300 volts was the trend in the curve. Iodine seemed to favor the high voltages by not dropping off as severely as xenon. Considering this trend, if the data

were projected forward to higher voltage, the gap between the propellants would grow, making iodine an even more attractive option.

The data shown in black is labeled “Busek I” because the data was not taken by the author, but in a separate set of tests by Busek Co. The Busek data was taken one day before the author’s data. These test points will therefore not be considered in the analysis below. The data is shown for comparison only. It is interesting to note, however, that the Busek data is consistently higher than the author’s iodine points, but they have identical trends for all performance parameters. There are a number of factors that could have influenced this. Mass flow calibrations and measurements are a strong possibility. This would not change thrust though. Thrust to power data differences can only be explained by different measurements of thrust or discharge conditions. The other possibility is a difference in thruster operation at high mass flow. The lower mass flow Busek data is much better correlated to the author’s data.

Specific impulse trends were similar to thrust to power. Xenon results appeared typical for this thruster [14]. Specific impulses ranged from about 1100 seconds to 1750 seconds on xenon and 900 to 1850 on iodine. Specific impulse is frequently correlated to thrust to power ratio. This was done to give a visual of the tradeoffs made in selecting an operating point. As a result, the iodine and xenon data did not have the same range of conditions. Therefore, the large range of iodine specific impulses was more impressive since it has less variability in thrust to power. The charts are also less intuitive when thinking in terms of power. High thrust-to-power numbers occurred at lower discharge voltages, therefore it is more intuitive to transpose the horizontal axis. Iodine outperformed by xenon for most of the range. The maximum gap was about 10% in

favor of xenon at the high thrust to power ratios. As with thrust, xenon looked better at low power. The iodine does seemed to overtake xenon at higher power. The crossover occurred very close to the xenon nominal operating condition of 200 watts. When examined 300 volts, the average specific impulses only favored xenon by 2.98%. So, the trade for running iodine instead of xenon was 12% more thrust for 3% less specific impulse. The specific impulse trend appears steeper for iodine, which could mean superior specific impulse is possible at higher power levels than examined in this study. The iodine curve shows no sign of peaking as xenon does at the low thrust-to-power ratios. Although the Busek data is not considered, the curves follow one another closely. This data suggest continued specific impulse gains at high discharge voltages.

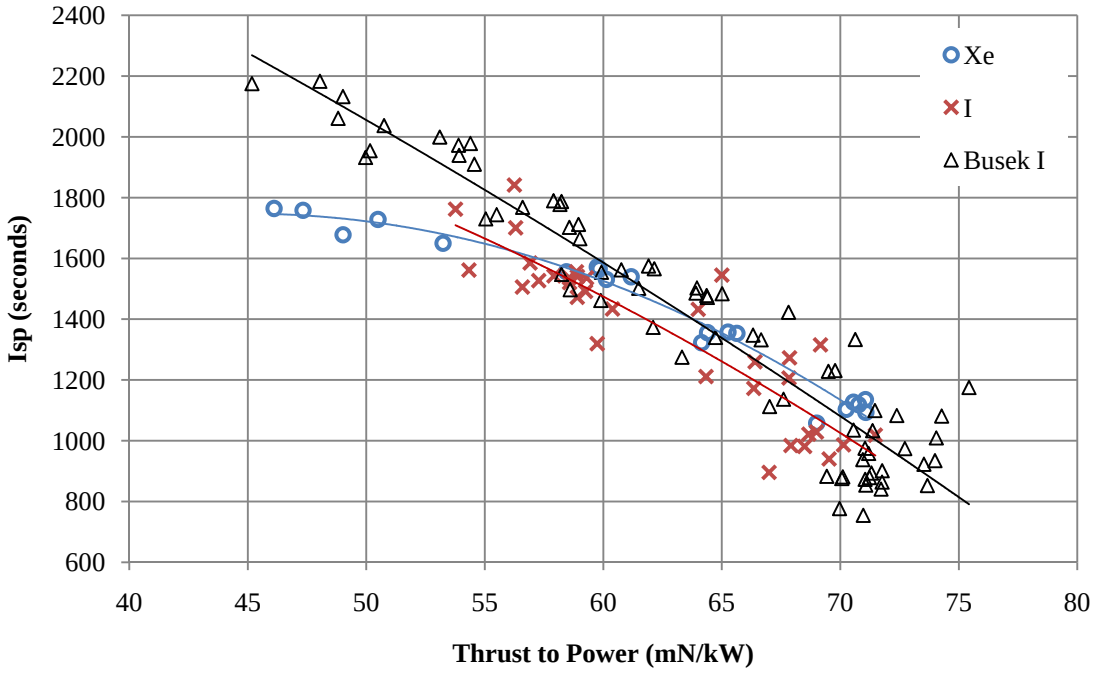

Figure 23: Specific impulse for iodine and xenon compared with Busek data

The specific impulse draws attention to the uncertainty in mass flow measurements. The xenon data was well correlated and had relatively low error. The

iodine data had a large variance since the xenon flow system was a commercial off the shelf system while iodine mass flow varied widely. The best correlated data was near 250 volts, the nominal condition, where the system was calibrated. This included most of the data between 55 and 65 milli-Newtons per kilowatt.

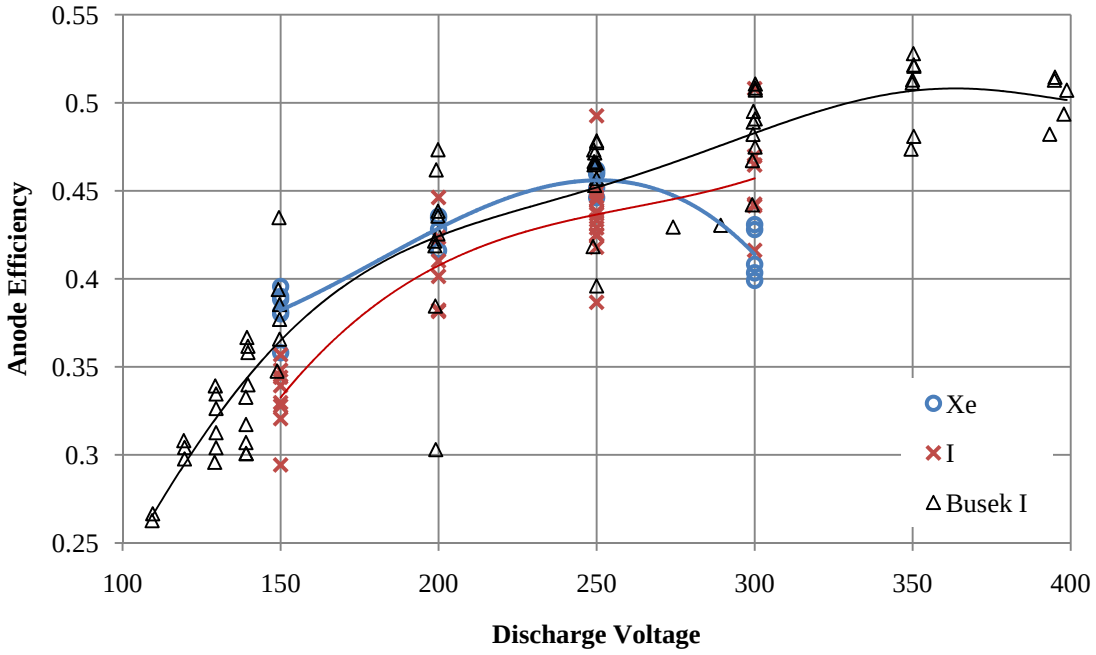

Figure 24: Anode total efficiency for xenon and iodine compared with Busek data

The total anode efficiency numbers were the final performance characteristic examined. Xenon results were again typical ranging from 38% to 46% . Iodine results as with specific impulse varied widely from 32% to 51%. However, the highest average efficiency for iodine was only about 46% at 300 volts. As with the other performance numbers, iodine was outperformed by xenon at low voltage levels and surpassed xenon at high voltage. The xenon efficiency peaks at 250 volts. This was an encouraging result, since the thruster was designed to be the most efficient at its operating point. The iodine

appeared to be reaching an approximate peak efficiency at 300 volts. The average efficiencies at the most efficient voltage are roughly equivalent at 46%.

The large variance in iodine data points was most likely due to mass flow as before. The data suggested there is a dependence on another variable, but there seemed to be no correlation upon examination. In actuality, the variations looked more like noise in the iodine feed system. Future efforts should rely on a more accurate and precise feed system in order to make better comparisons.

The iodine had comparable performance to xenon. However, at the thruster nominal condition of 250 volts, xenon had the clear advantage. On the other hand, iodine was higher performing all around at 300 volts.

This is an exciting result for the future of electric propulsion. Running iodine at high voltage increases thrust without sacrificing efficiency or specific impulse. Another highly studied Hall thruster is the BHT-1500. It is a 1.5 kilowatt thruster capable of running higher voltages safely. On this thruster, the potential exists for iodine to outperform xenon in every performance category. Additionally, iodine seems to run better at high power on the same size thruster. This means that thrusters designed for iodine can be smaller than those designed for xenon, assuming the design power is the same. Even on the 200 Watt thruster, the high thrust delivers an important advantage. Higher thrust means decreased flight time. Decreases in flight time become more important as missions get longer. Future missions will require this advantage.

The performance measurements revealed iodine to be a high performing propellant. Iodine looked similar to xenon in most cases, but surpassed it in the high

power range. The plume measurements confirmed the performance data and gave some insight into what mechanisms are causing the gains.

IV.3 Faraday Results

Performance measurements told a lot about the overall performance of a thruster. They provided useful numbers for comparison, like efficiency. However, performance measurements provided no insight into how the power is lost. Faraday measurements helped determine several loss mechanisms, including plume divergence, current fraction, and mass fraction. Each operating condition tested in the performance measurements had a corresponding Faraday sweep.

Since the Faraday probe was a nude design, the charge exchange ions were apparent in every sweep. Additionally, iodine and xenon operated at different background pressures. This was expected since iodine had a lower partial pressure than xenon at room temperature. The difference was almost a factor of two. In order to compare iodine and xenon more effectively, the charge exchange wings were removed. The technique used was outlined by Azziz [15]. The xenon and iodine Faraday curves were assumed to drop off exponentially with the angle off centerline, resulting in a straight line on a log scale. This correction more accurately predicted what the thruster was doing since the wings form downstream of the thruster face, well after the momentum exchange has occurred. All calculations are based on the corrected data rather than the raw data.

Figure 25 shows an example corrected Faraday curve with the uncorrected data. The current density is plotted again Faraday probe arm sweep angle. This should

produce an approximately exponential decrease in current density. The corrected data follows the slow of the actual data prior to the presence of charge exchange ions, suggesting the method used is accurately predicting plume model.

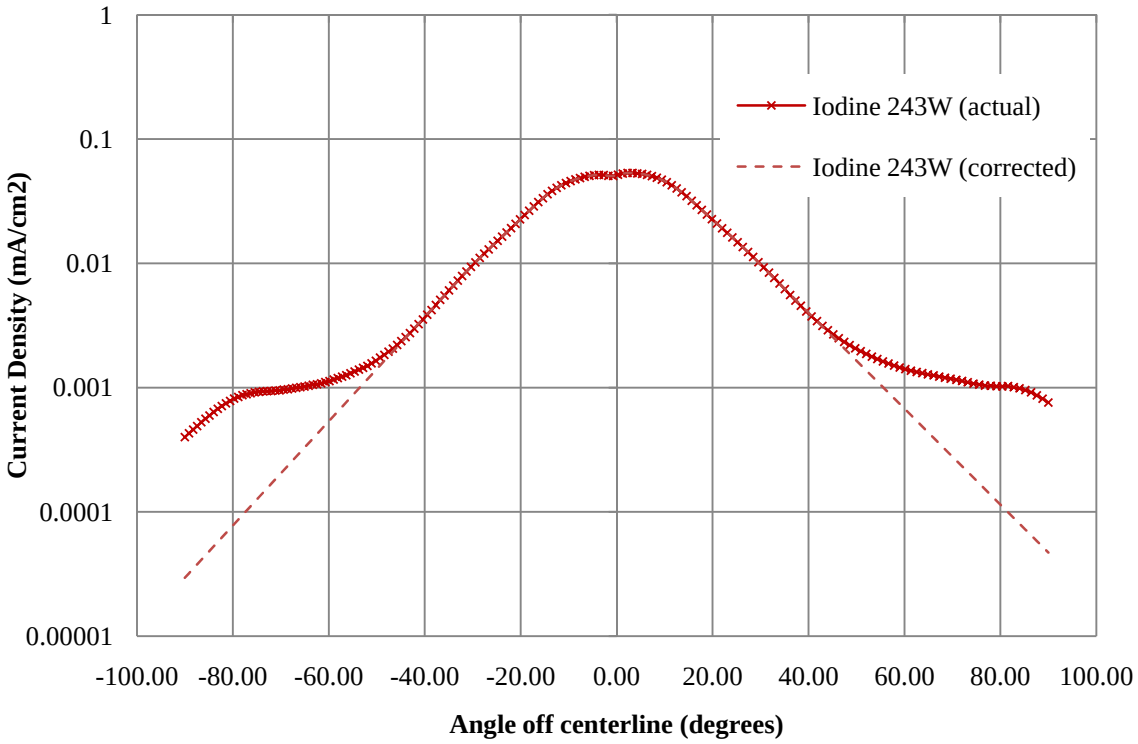

Figure 25: Faraday sweep correction for charge exchange wings

The Faraday sweeps showed more collimated iodine peaks at every test voltage. The xenon had larger wings suggesting some more losses than the iodine. The larger xenon wings point to better directional efficiency for iodine rather than increased current in the iodine plume. However, all of these arguments were artificial, since the background pressure was higher for xenon creating more charge exchange ions. Therefore, all Faraday data shown has been corrected for charge exchange wings for more valid comparison. Once this correction was applied, the results still showed larger wings in the xenon plume. At about 30 degrees off centerline and continuing out in each

of the sweeps, xenon has higher current density. This reinforces the original hypothesis that iodine has superior directional efficiency.

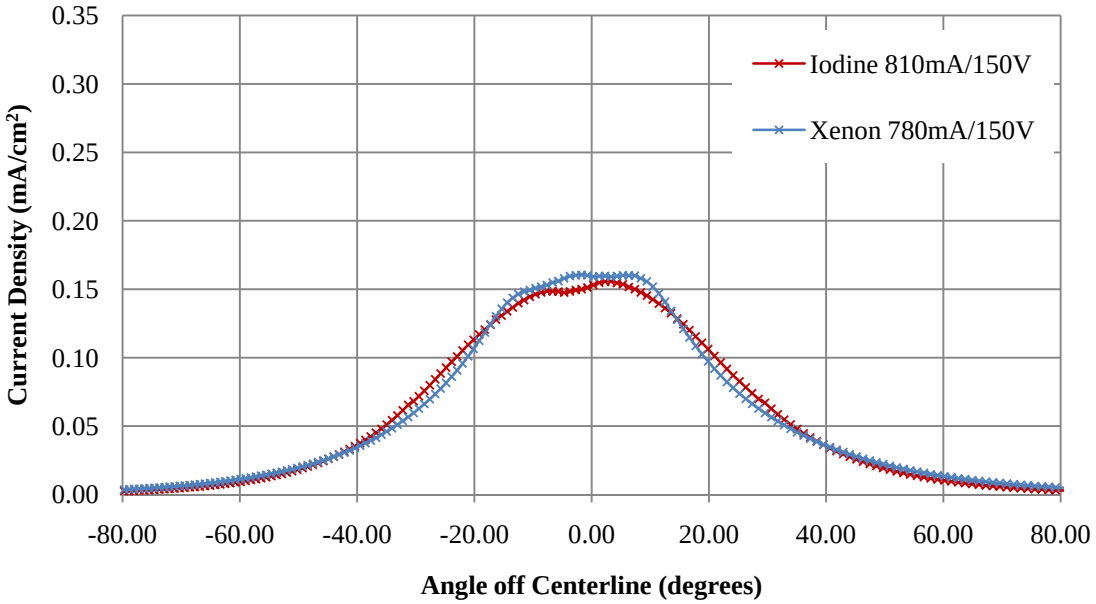

Figure 26: Corrected Faraday data for xenon and iodine at 150 volts discharge

Figure 26 represents the Faraday data for xenon and iodine running at 150 volts discharge potential. This conditions shows the two propellants to be very similar In fact, the xenon even peaks higher than the iodine. However, the iodine still is more concentrated near the center. Between 20 and 40 degrees off the centerline, the xenon lacks in current density. The remaining current in the xenon ends up in the wings beyond 40 degrees off centerline.

Figure 27 compares iodine and xenon Faraday sweeps at 200 volts discharge potential. The difference is much more readily apparent in this figure. The iodine is significantly more concentrated near the centerline, and at 30 degrees the xenon begins becomes more concentrated. This is all evidence of higher directional efficiency for iodine.

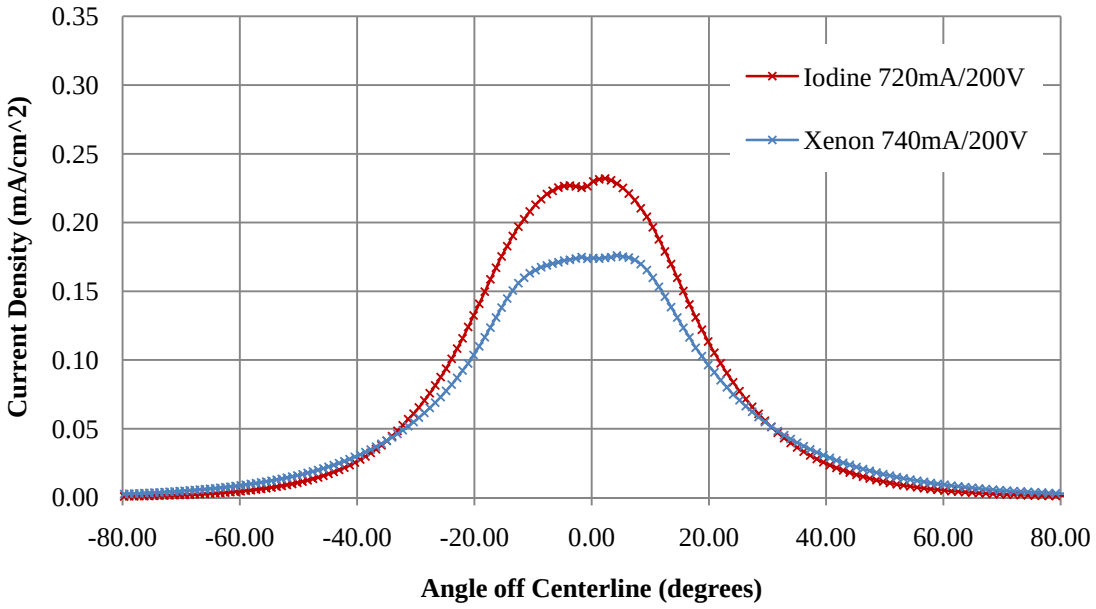

Figure 27: Corrected Faraday data for xenon and iodine at 200 volts discharge

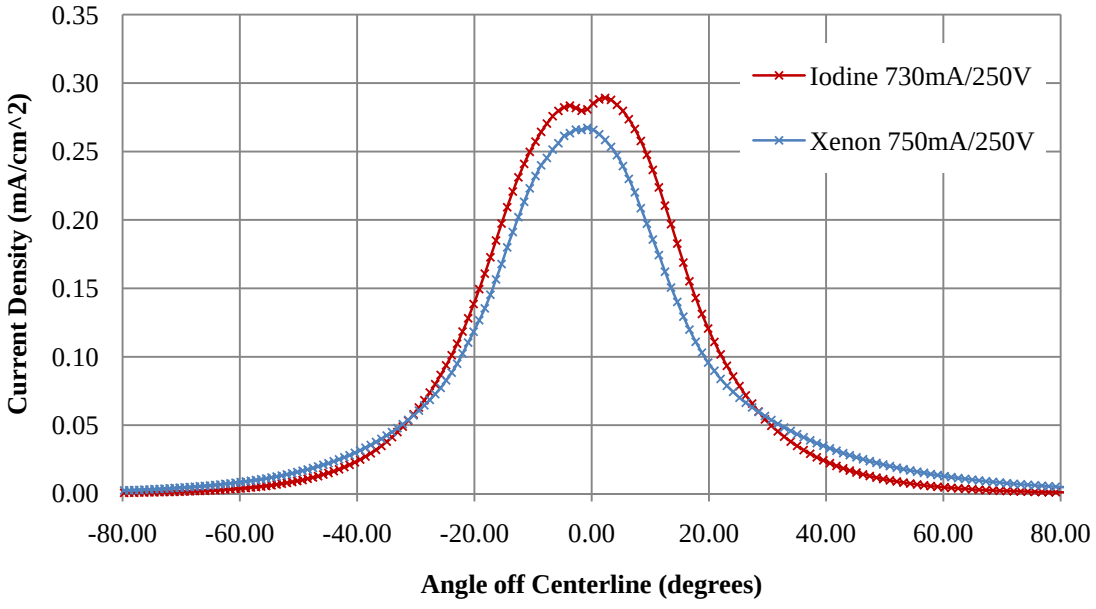

Figure 28: Corrected Faraday data for xenon and iodine at 250 volts discharge

Figure 28 displays the 250 volts discharge potential Faraday sweeps for iodine and xenon. At 250 volts, the xenon begins to look more directional. This is expected since the thruster is designed around this condition for xenon. The iodine, however, is still more directional, crossing over the xenon current density at around 30 degrees.

Figure 29 shows the final Faraday sweep discharge potential of 300 volts. This is the most severe difference between the two propellants. Iodine is considerably more concentrated along the thrust axis. Again, the cross over in current density occurs around 30 degrees off axis. This time the cross over is more pronounced. The iodine is almost negligible beyond 60 degrees, while the xenon remains significant across the profile.

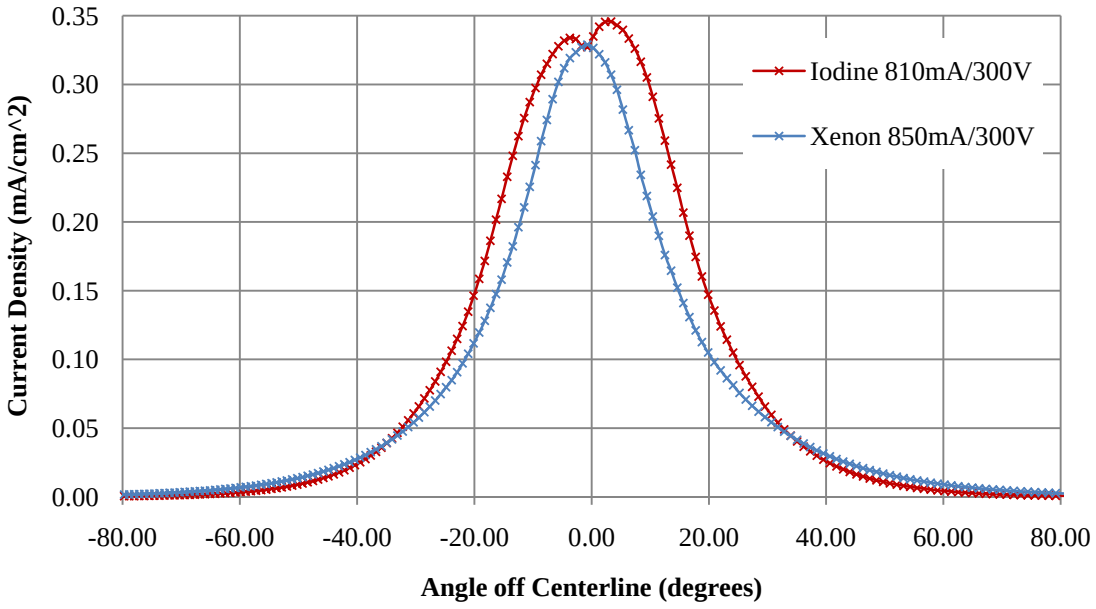

Figure 29: Corrected Faraday data for xenon and iodine at 300 volts discharge

The directional efficiency was calculated from the Faraday data. Some ExB probe data was included in this calculation. Since the ExB data did not need to be corrected for background pressure, the comparison was valid. The directional efficiency calculations were performed for both corrected and uncorrected Faraday data.

Figure 30 shows the directional efficiency for each propellant at various discharge potentials. The charge exchange wings have been removed in the corrected data, and left for comparison in the measured data. The solid lines represent the trends for the uncorrected data, while the dotted lines represent trends for the corrected data. The difference is much more severe for the uncorrected data. The corrected data still shows a clear iodine advantage at all conditions measured. There is very low variance in the data, supporting the experimental setup and methodology used to reduce the Faraday data.

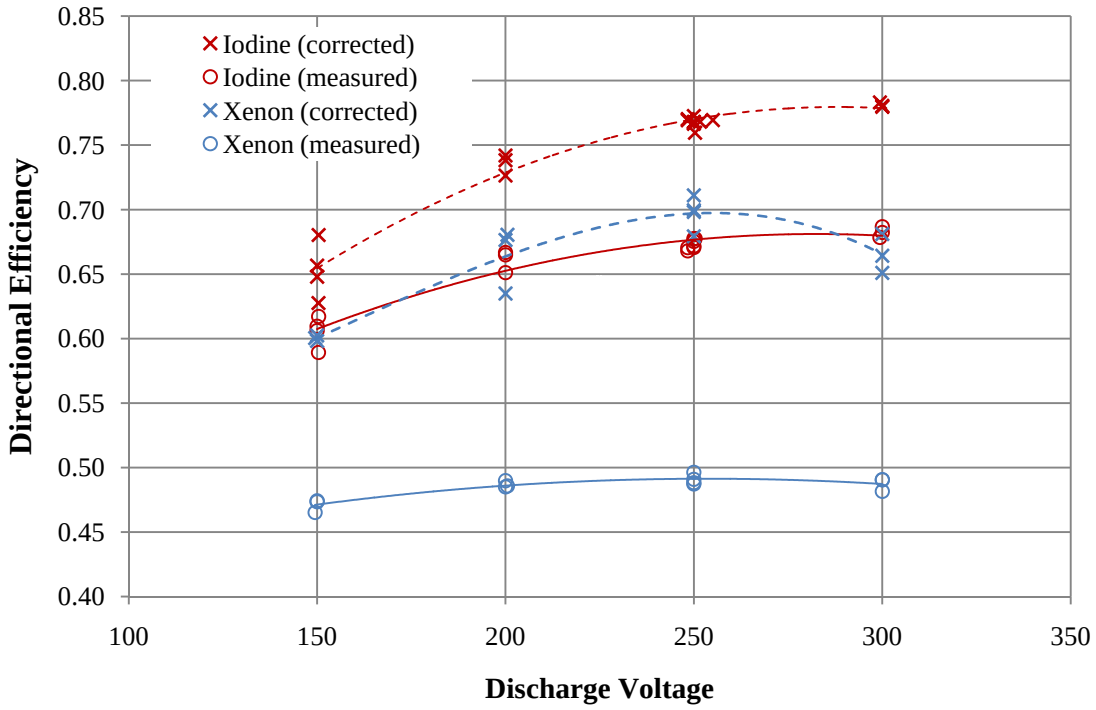

Figure 30: Directional efficiency, γ^2, for xenon and iodine

The directional efficiency of iodine was the main reason for the superior efficiency at high voltage and reasonably high efficiency at all conditions. Even though xenon was more radically corrected for charge exchange ions, iodine was more

directionally efficient. Even at 150 volts, iodine was about 8% more efficient. The xenon reached a peak condition near the operating point averaging 70% efficiency. This still accounted for the largest of the anode losses. The iodine peaked at 300 volts as expected with a directional efficiency averaging 78%. This was 16% better performing than xenon.

The current ratio, η_b, was calculated from the comparison of the Faraday integrations and the PPU output discharge current. This current integration technique was highlighted in chapter 3. The current ratios were found for the high and low current settings at all test voltages.

Finally, the Faraday probe was used to estimate ion mass flow rate. This was compared to the propellant for rate for the mass efficiency. The ExB was used to determine the species. The species concentrations and currents were used in conjunction with the Faraday data to find the mass efficiencies as with the directional efficiency. The Faraday probe data revealed a great deal of the information about the plume, the ExB probe made the Faraday probe data more useful and found the remaining terms in the efficiency calculation.

IV.4 ExB Results

The function of the probe was to find the current for ions of various energies in the ion discharge. Included in the energy is the velocity, charge state, and mass. This information was used to convert current to mass flow, relating the plume measurements to performance. For typical propellants, like xenon, mass was constant. This was not the case for iodine, making data reduction a bit more difficult. When examining the data, the

velocity distribution was much less of a factor than the charge state, creating distinct peaks that were assumed not to interfere with one another. Xenon peaks occurred at distinct point based on the charge state, Iodine, however, has theoretical overlaps. I^+, theoretically, is measured at the same location as I_2^{2+}, but I_2^{2+} is not a stable species. It can therefore be assumed that it does not exist in any appreciable amount in the plume. This leaves only four significant species to look for which do not overlap.

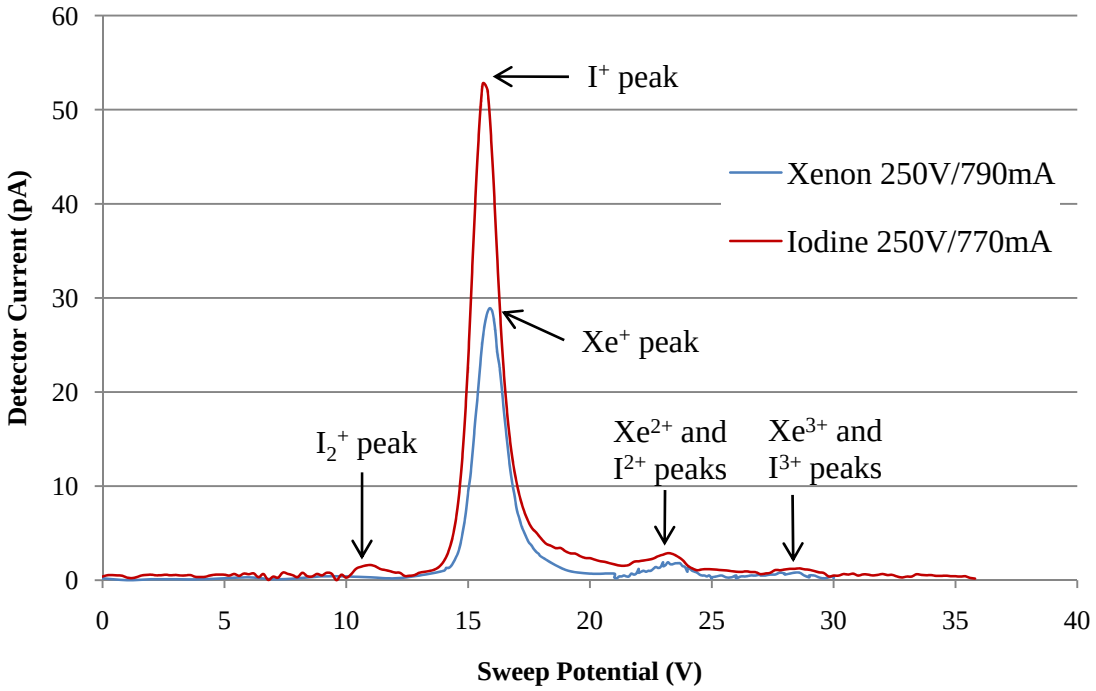

Figure 31: ExB raw data for xenon and iodine at 250 volts

The xenon peaks appear typical. The ion fractions and current fractions were calculated from the maximum value at the peaks by using equation 30. The ion current at the peak is equal to measured current assuming no secondary emissions.

$$\Omega_i = \frac{I_i}{\sum I_i} \quad \text{i = peak number} \tag{30}$$

The current fractions are useful, but mole fractions are the more commonly displayed result. The current is found with the number densities and the properties of the species as in equation 31

$$I_i = (eq_i)^{3/2}\, n_i \sqrt{\frac{2q_i eV_d}{m_i}} \tag{31}$$

Using this relationship inserted into equation 30 reveals a way to find mole or number fraction in equation 32

$$\zeta_i = \frac{n_i}{\sum n_i} = \frac{{\Omega_i m_i}/{q_i^{3/2}}}{\sum {\Omega_i m_i}/{q_i^{3/2}}} \tag{32}$$

This mole fractions can be determined from the current measured by the device and knowledge of what species is being reduced. In this case, both are known [20].

Table 2 gives the mole fractions reduced in this way. The xenon has more of the singly ionized monatomic ions than iodine. This would be a concern, but the more desirable diatomic iodine ions more than offset this. The 2.9% diatomic ions in the plume, more than the difference between I^+ and Xe^+, provide a significant advantage for iodine. This results in higher efficiencies from ionization fractions for iodine.

Table 2: Xenon and iodine species mole fractions at 250 volts

Species	Mole Fraction	Species	Mole Fraction
$I_2{}^+$	0.029	Xe^+	0.975
I^+	0.953	Xe^{2+}	0.021
I^{2+}	0.015	Xe^{3+}	0.004
I^{3+}	0.003		

The iodine reduction was not surprising. Since the thrust was not double the thrust of xenon, the diatomic iodine peak could not be as large as the monatomic iodine peaks. The xenon results were similar to previous studies. The iodine fractions were fairly close to the xenon fractions excluding the diatomic species. This explained the approximately even performance numbers displayed by both propellants at this operating condition.

From the ExB data, the α term in the directional efficiency was determined. α for xenon at 250 volts is 0.976. For iodine at 250 volts, it was 0.99 on average. This is not a significant difference between the two. This indicates that the main difference in the directional efficiency comes from the directionality rather than the species in the plume. Another term was calculated from the ExB data in order to find mass efficiency. Ion mass flow was calculated by using the current fraction data and dividing out the charge state. This correction factor allowed for ion mass flow to be calculated as if all ions were one species. Unfortunately, the ion mass flows were higher than the actual propellant flow for all of the xenon test points. This is physically impossible by conservation of mass, so 100% was set as a ceiling for this efficiency. The iodine numbers on the other hand were reasonable, ranging from 80% to 95% efficient at 250 volts.

The location of the peaks was just as important as the magnitude. The ion velocities were taken from the peak locations using the ExB probe specifications. Assuming the ion was accelerated purely from the potential applied to it in the thruster, the average voltage at the ionization zone was estimated. This was more true for the first ionization states since the higher order ions changed ionization state at two different potentials in the plume. This allowed for direct calculation of the discharge voltage ratio.

The voltage efficiency for xenon was 91.5%, while the average for iodine was 88.9%. Xenon is apparently more effective at ionizing earlier in the channel. This was likely due to the iodine dissociating more often than ionizing upon first electron impact, and therefore diffusing further before becoming ionized. This effect did not dominate to the efficiency, but was significant.

IV.5 Efficiency Comparison

All of the anode efficiency terms were calculated individually for the 250 volt discharge voltage case. The calculated plume efficiencies were compared to the performance measurement efficiencies. The iodine and xenon measurements were exceptionally well correlated with the plume measurements. The iodine plume measurements averaged only 0.4% higher efficiency than the performance measurements. This is an important verification of the performance data. The xenon plume average efficiency was only 2% higher than the performance average efficiency. This validates the methods used on a known propellant. The greater uncertainty in the xenon data came from the method used to exclude charge exchange ions. Small variations in the slopes chosen by the author have a significant impact on this data. Xenon, operating at higher chamber pressure was more vulnerable to this effect.

Figure 32 shows all efficiencies for plume and performance data at 250 volts discharge potential. Incredibly, the two completely separate tests closely agree on the final anode efficiency. The efficiencies shown against discharge current, since the voltage is constant in this case.

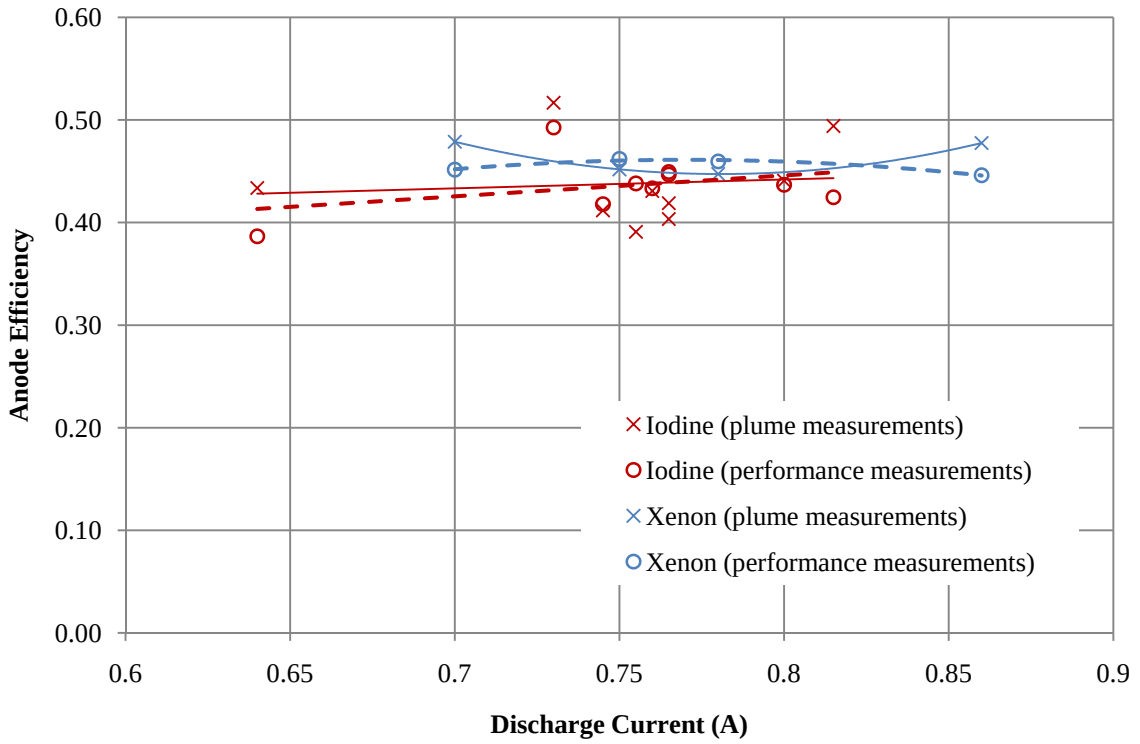

Figure 32: Comparison of plume and performance efficiencies at 250 volts discharge

For data points not at 250 volts discharge, the same ion species fractions and voltage efficiencies were assumed. Figure 33 shows the estimated plume efficiencies compared to the performance efficiencies for the entire experiment. This data is not meant to be correct, but it is a tool and a sanity check. They should not be the same since the ExB data is expected to be different at this condition. The iodine data is still very close correlated. This means iodine species fractions don't change significantly with discharge potential. Conversely, xenon diverges quickly from the performance measurements. Xenon is estimate to be more efficient than it actually is at discharge potentials other than 250 volts. This is an encouraging result. The design point is at 250 volts, so this should be the best performance location. Therefore, using this performance elsewhere gives aggressive results. The ion fractions should actually be less than optimal

off design point. This would be the plume curve back down to the performance curve in theory.

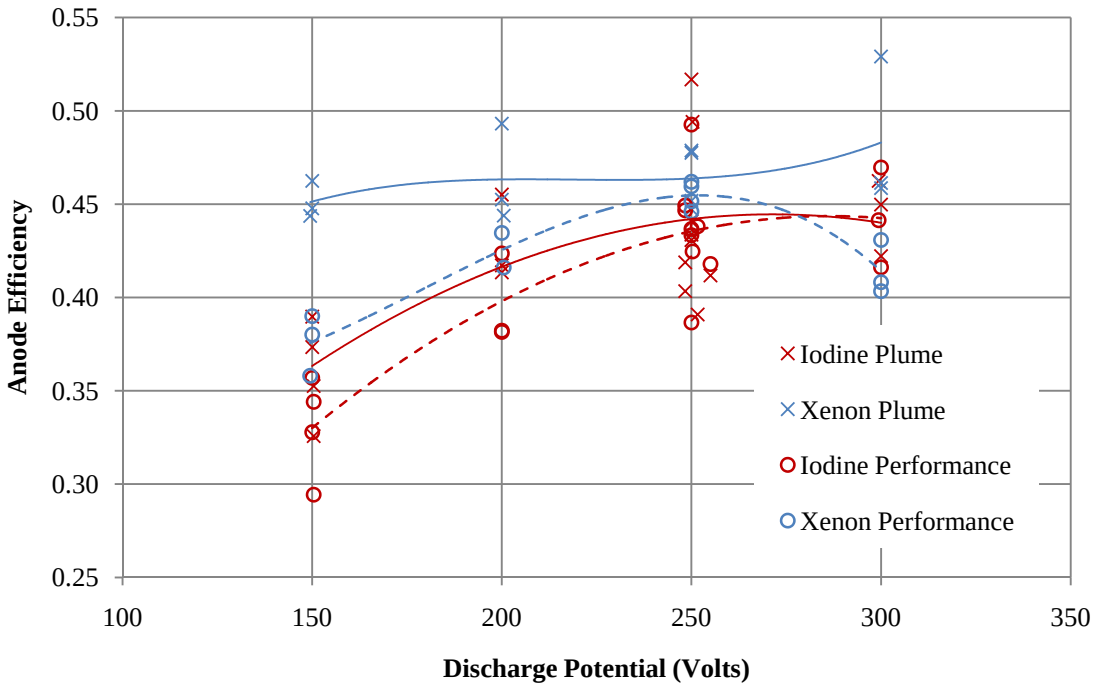

Figure 33: Anode efficiency comparison of projected plume measurements and performance measurements for xenon and iodine

All of the conventional efficiencies needed to compare thrusters and propellants were used in the analysis. However, an unconventional efficiency was needed to fully compare the two propellants.

IV.6 Power Analysis

A major flaw in direct comparison between xenon and iodine efficiencies was that iodine required heating to become a gas and remain a gas until flowing out of the thruster. To compare iodine to xenon, an efficiency term was introduced.

$$\eta_h = \frac{P_t}{P_t + P_h} \tag{33}$$

P_t was the power consumed by the thruster, and P_h was the power used to heat the iodine. The PPU power was used in this analysis for P_t. To estimate heater power some assumptions were needed. First, 10% efficiency was assumed in the heating process as a conservative value. This accounted for the losses from heat transfer and the energy losses in the heaters themselves. Also, a mass flow rate of one milligram per second was assumed. This was higher than any test point taken to be conservative. Then, enthalpy curve fits and latent heat of sublimation for iodine were taken from NIST Chemistry Webbook [21]. These values allowed for the estimation of P_h, which was about 2.6 Watts. Then, the heating efficiency was calculated using this power for a range of thruster power levels. Assuming heater power to be a constant is not a great assumption since mass flow fluctuated with thruster operating condition, but high values for mass flow were used so that all values could be considered conservative. The efficiencies calculated were plotted in Figure 34.

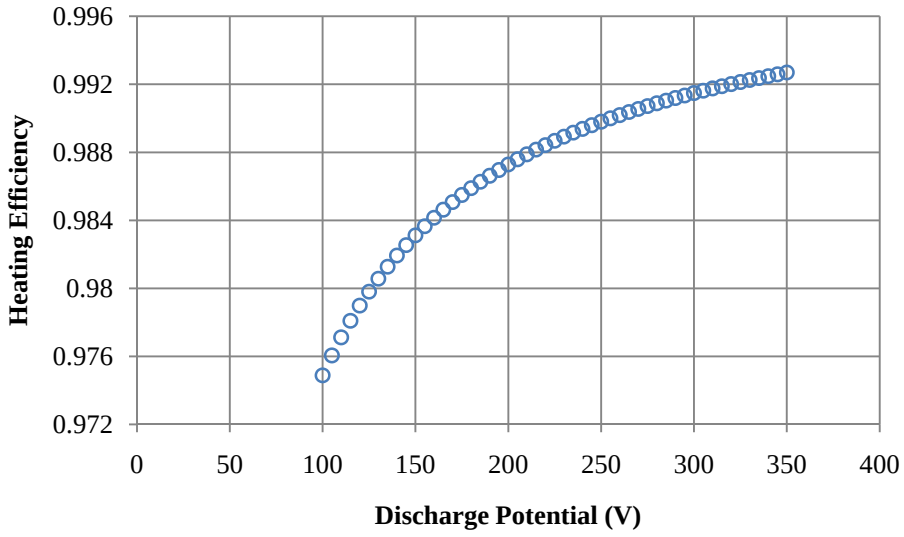

Figure 34: Heating efficiency as a function of discharge volatage

The efficiencies found in this exercise were minute when compared to other thruster losses. The heating of propellants was concluded to be much more of a complexity issue than an efficiency issue. Additional issues arose when examining components used with iodine.

IV.7 Part Degradation and Complications

As with any new research, there were a number of complications in switching to iodine. The purpose of this section is to address the more qualitative losses in switching to iodine. Once the iodine feed system first running, the thruster was run at several conditions to verify the thruster worked and thrust was produced. This included high discharge voltages and flow rates. Upon examination, the anode had melted significantly. The decision following the incident was to run at 300 volts maximum for the remaining research. It was not evident at what power setting the anode began to melt, so 300 volts was chosen as a conservative value.

Figure 35 shows and axial view of an installed anode shortly after operation ceased. This anode was operated at too high of a power for this experiment, resulting in eventual failure of the anode itself. This is a serious concern for space thrusters trying to run iodine. It may be that early testing just pushed the ability of the thruster too far. If this was the case, xenon operated at the identical conditions would have produced similar results. On the other hand, this could have been a side effect of an iodine fueled Hall thruster. If the latter is true, separate guidelines must be established to safely operate the thruster in future tests and missions.

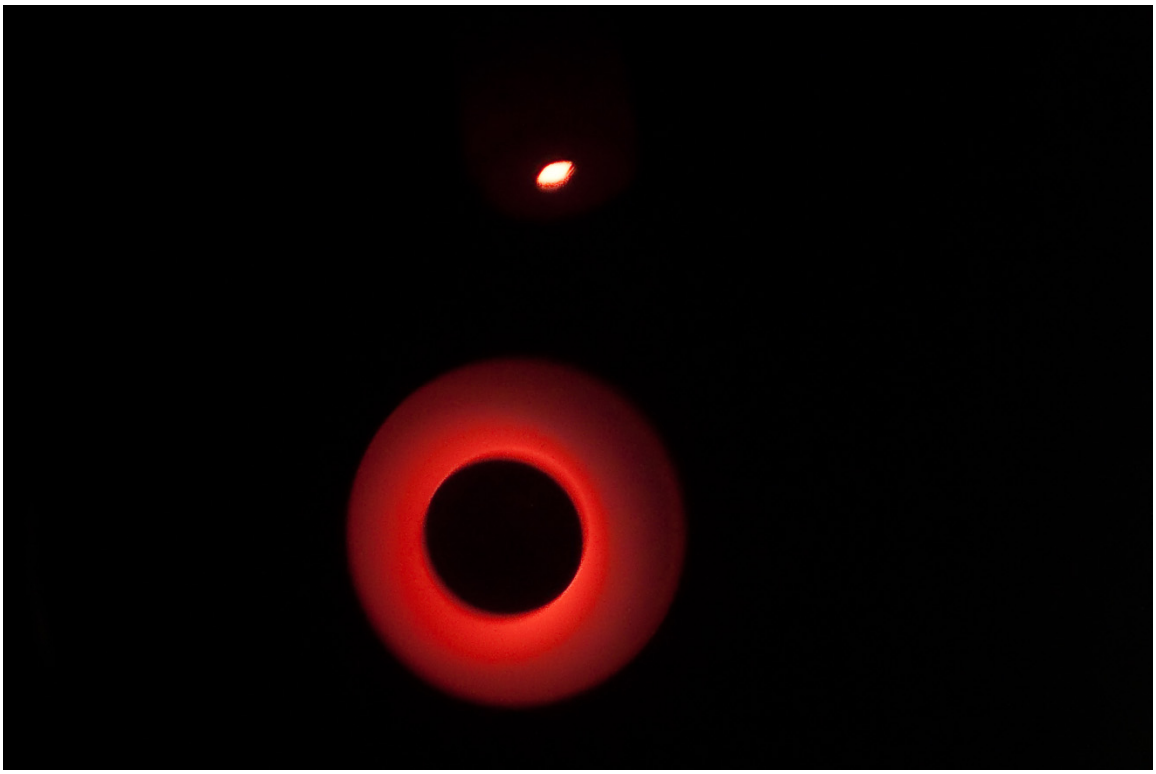

Figure 35: Glowing hot anode just after turning off thruster

Each time a component that was exposed to the hot iodine was removed, there was no significant discoloration. However, when the component was exposed to atmosphere for several hours, significant oxidation occurred. It was unclear what mechanism is causing this, but the result was consistent.

The first and second anodes, shown in Figure 36 and Figure 37, were operated at high voltage and discharge current. The first anode was exposed directly to oxygen after operation. The second anode was allowed to soak in nitrogen gas in the tank while cooling down and was operated less aggressively. Both anodes appear to be rusted beyond usability. No tests were performed on the anodes to look for iodine.

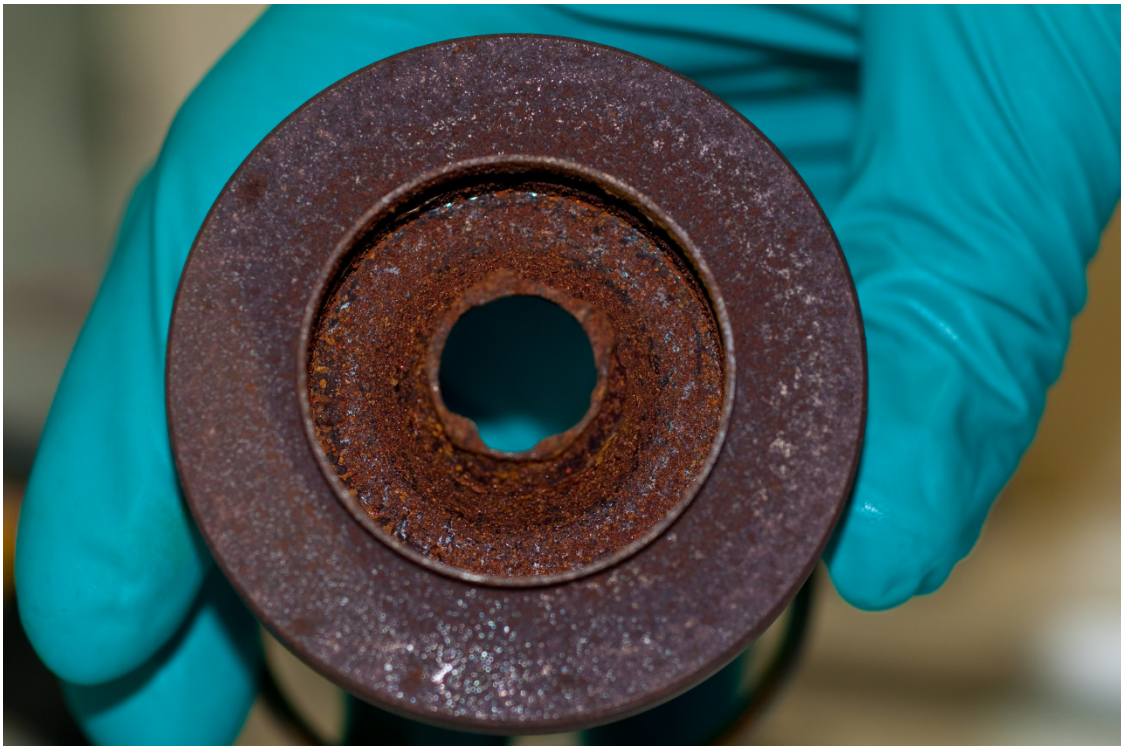

Figure 36: Melted and severely oxidized anode, first anode used

Figure 37: Melted anode showing less oxidation, second anode used

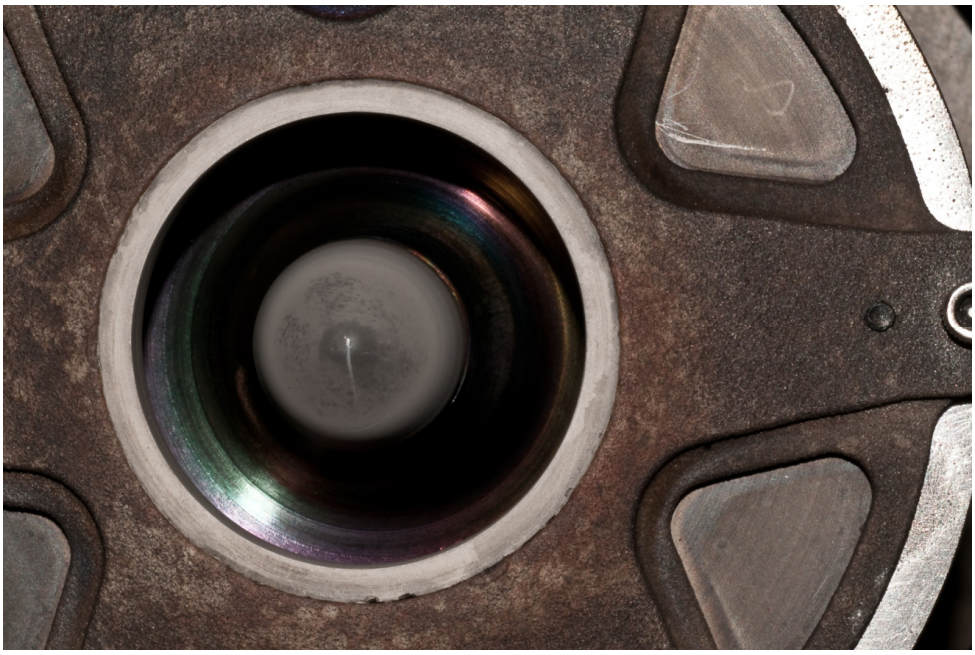

Figure 38: Third anode installed before operating on iodine

Figure 39: Third anode used after 20 hours of operation on iodine (still operational)

The third anode, shown in Figure 38, was never operated above 300 watts and remains operational despite some solid buildup shown in Figure 39. The thrusters were most severely affected by the hot iodine, but other components were damaged along the flow path.

The iodine feed lines were heated as uniformly as possible. Components in the line, like valves, were also completely wrapped with heater lines. It is extremely difficult to maintain a high enough temperature inside these components to avoid deposition. The first attempt to control the flow involved a flow controller downstream of the reservoir, valves, and pressure transducer. This allowed for excess iodine to build up behind the flow controller. The advantage of this system is immediate control over the discharge condition since excess pressure is always available. This system proved problematic because it required higher heating between the reservoir and the flow controller. If the temperature is not hot enough, the iodine will find the cold spots and begin to deposit. Eventually these deposits will form complete clogs in the system causing the thruster to shut off. As long as the reservoir pressure is not brought up too high and the temperature is higher at other locations, this should not be an issue.

Figure 40 illustrates a significant iodine buildup in the feed line. The iodine buildup did not cause a direct blockage in this case, but the valve no longer functioned, essentially resulting in a blockage. Figure 41 on the other hand shows a complete blockage from iodine buildup. The blockage could only be cleared with copious amounts of acetone.

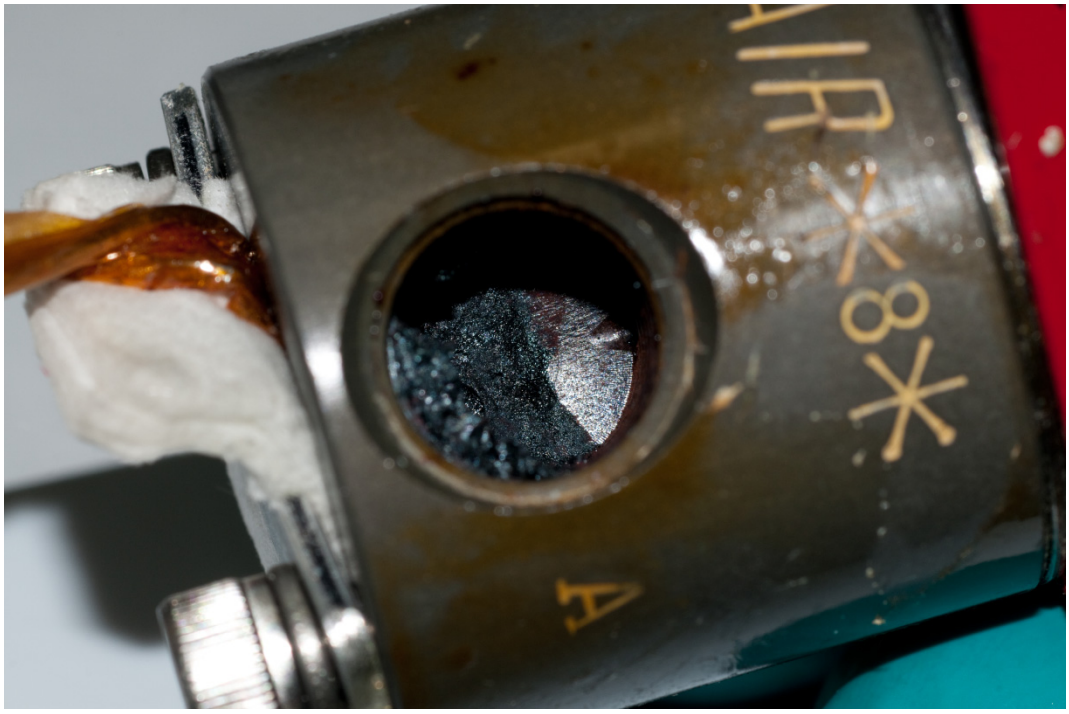

Figure 40: Three-way valve with iodine deposits

Figure 41: Total blockage of iodine feed line

Another event that caused deposition was the thruster shutdown procedure. The procedure for shutting down the thruster was to run xenon for no less than one hour after running iodine to clear out the system while all the heaters are shut off. This technique was effective at keeping the thruster working, but not keeping the lines free of solid iodine. The best procedure was to run xenon through the thruster as before, then shut down the reservoir heater and let it cool to room temperature, effectively limiting the hot iodine deposition locations to the reservoir or the thruster exit. Then, the heater lines were shut down along with the thruster. This seemed to increase accuracy in mass flow the following day and limit problems in start up. The experience in resolving these issues eventually limited deposition issues.

Figure 42: Three-way valve oxidation after flowing hot iodine

Even with proper procedure and experience, iodine still corroded certain materials. Figure 42 shows the iodine corrosion of the 3-way valve. This side of the valve did not have iodine deposits on it at any time, but was significantly discolored after exposure to atmosphere. This may have been avoided with less heating of this particular component, but that risks deposition.

There are valuable lessons learned in the results of this experiment. Iodine fueled Hall thrust operation is tricky in several ways, but the challenges can be overcome with experience. There is motivation to do so. Iodine has desirable efficiency, thrust, and specific impulse at high power. The data is strong and was validated by separate instrumentation. This propellant should be explored further and will achieve real world gains.

V. Conclusions and Recommendations

Electric propulsion is an important capability for the future of space missions. Many of these devices use xenon as a propellant. The propellant is proven and has many desirable properties. However, xenon performance is limited. Some limitations include ionization energy and molecular mass. Additionally, world xenon supply is dwindling, and prices are climbing. Iodine is one of the possible replacement propellants. Iodine has many properties desirable for an electric thruster propellant. As shown in Chapter 4, practical iodine fueled Hall thrusters can be operated without modification to the thrusters, and with a cheap and simple feed system.

Iodine performance is similar to xenon with some superior qualities at high voltages. Iodine is able to produce comparable thrust to power to xenon at all conditions and exceeds xenon at 300 volts. The most likely cause of this is the directionality in the plume. The iodine is far less likely to spread out from the thruster face, thereby losing some momentum transfer capability. Specific impulse is lower for iodine at most conditions but reaches xenon performance levels at higher voltages. Trends in iodine specific impulse suggest a higher specific impulse than xenon is likely at low thrust to power settings, or higher voltages than 300. Efficiency again is comparable to xenon at most operating conditions. Directional efficiency is substantially increased for iodine, but mass efficiency is decreased. These terms somewhat balance each other out creating the similarity between the propellants. Maximum efficiency is approximately equal for both, but xenon peaks at 250 volts while the maximum efficiency for iodine is observed at 300 volts. The efficiency does not decrease with increasing discharge potential over the tested region. The peak efficiency for iodine may be greater than xenon at discharge

potentials than 300 volts, although there appears to be an approximate peak forming. Table 3 outlines the performance numbers measured in this experiment.

Table 3: Measured performance for various operating conditions

Voltage	150		200		250		300	
Propellant	Iodine	Xenon	Iodine	Xenon	Iodine	Xenon	Iodine	Xenon
$T/_P$ (mN/kW)	69.0	70.4	67.0	64.8	59.6	59.7	56.0	49.0
I_{sp} (sec)	982	1106	1240	1347	1494	1553	1665	1716
η_T	33.3%	38.2%	40.8%	42.9%	43.7%	45.6%	45.7%	41.4%

Table 4: Measured efficiencies in the plume

Voltage	150 Volts		200 Volts		250 Volts		300 Volts	
Propellant	Xenon	Iodine	Xenon	Iodine	Xenon	Iodine	Xenon	Iodine
η_b	78.4%	75.4%	76.2%	77.5%	74.1%	75.1%	74.0%	80.5%
η_v	-	-	-	-	91.5%	88.9%	-	-
η_m	104.8%	82.4%	100.2%	84.6%	98.1%	85.3%	107.3%	92.3%
α	-	-	-	-	97.6%	99.0%	-	-
F_t	79.4%	81.6%	83.5%	86.6%	85.6%	88.5%	83.6%	89.3%
γ^2	-	-	-	-	69.7%	76.8%	-	-
η_T	-	-	-	-	46.4%	43.8%	-	-
η_T	37.6%	33.1%	42.5%	39.6%	45.5%	43.6%	41.4%	44.2%

Plume data closely agrees with performance data on efficiency. The main differences were in directional efficiency and mass efficiency. For xenon, off design

point, mass efficiency was significantly overestimated. Since the ExB data was applied to all voltage based on the 250 volt case, all the calculations assumed an overly ideal condition of species fractions. The mass efficiencies for this reason were reasonable, and would decrease if actual ExB data were taken. Table 4 shows all the efficiencies that were calculated based on plume measurements and compares the total anode efficiency from plume measurements and performance measurements.

Additional studies revealed iodine heating is not a significant loss. At nominal conditions, 99% of the power goes to the thruster and only 1% to the heater system. This is based on conservative estimates for the on orbit system.

The degradation of components used to run iodine is a major issue. However, the issues only seemed to come about after the system was exposed to atmosphere – more specifically oxygen. This is an issue for ground testing, but not nearly as much in space. If the thruster is properly tested and maintained in a nitrogen environment or coated for protection, this issue can be avoided. However, it should be the subject of future research.

The mass flow system used in this experiment was good for first order comparisons. Although enough data was taken to calculate confident averages in this experiment, future tests should not have to rely on brute force to get results. A better mass flow system is needed for precise control over the mass flow. The measurements were based on absolute pressure upstream of the thruster. Pressure is not linear with mass flow, nor is mass flow independent of operating condition. In fact, the same pressure and operating conditions may give a different mass flow on a different day, because of small blockages in the feed lines. A mass flow controller like the one used for

xenon is better for this experiment. It is important to note that the entire mass flow controller unit would need to be heated as hot as the rest of the feed lines, in this case 150 degrees C. This heating would be exceptionally difficult in atmosphere depending on the design of the controller. This challenge may be overcome by submerging the controller in an oil or mineral water bath. This would serve to heat the system uniformly. This bath could house the entire feed system up to the thruster excluding the reservoir, which needs to be at a different temperature. This may eliminate many of the heating complications seen in this experiment. To best simulate the heat transfer environment, this apparatus should be placed inside the vacuum chamber with the thruster. A possible complication would be difficulty in adjusting the mass flow. There would need to be significant automation and instrumentation capable of remote operation to make everything work as smoothly as xenon.

A major drawback the iodine system is the cathode operation. Since the cathodes ran on xenon, both propellants are needed in the current setup. There is still significant savings in storage since only 10% of the xenon is needed, but the system is more complex. Optimally, there would only be one propellant on board. Iodine and other alternate propellants may be a motivation for solid state cathode research. This would eliminate the dependence on xenon, significantly reducing complexity and weight.

The data shown in Table 4 has missing values. It is the recommendation of the author to fill in the gaps to better understand iodine operation. More specifically, the ExB probe needs to be used at conditions other than xenon nominal. In particular, the 300 volt condition would be particularly interesting to examine because of the efficiency increase of iodine. Additionally, ion densities are not constant in the plume, It would be

beneficial to see how concentrations change at different locations in the plume. Therefore, the instrument should be on a translations stage to get data from more angles and radii from the thruster face. The Faraday probe should also be used at more radii. The arm that swept the Faraday probe in this experiment had a fixed radius, severely limiting the amount of analysis that could be done.

The instrumentation upgrades would characterize the thruster to a high degree of accuracy and precision. However, thruster upgrades could more significantly impact performance. Iodine seems to prefer high voltage for optimal operation. The thruster needs to be operated at conditions around and above 300 volts to find peak performance. This may be more easily accomplished on a larger thruster like the BHT-1500. Iodine may outperform xenon more significantly on this system.

There is a lot to learn about this new propellant. More research is required to make this propellant flight worthy, but the motivations are clear. Iodine provides a decisive increase in performance at high discharge voltage and can perform similar to xenon at all conditions. Iodine is a strong candidate to replace xenon in high power electric propulsion systems.

Bibliography

[1] Humble, R., Henry, G., and Larson, W., Eds., *Space Propulsion Analysis and Design*, 1st ed. New York, NY: McGraw Hill, 1995.

[2] Astronautix.com. (n.d.) SPT-100 Hall. [online database]. https://www.astronautix.com/engines/spt100.htm [cited 1 Mar 2011].

[3] Kieckhafer, A., and King, L. B., "Energetics of Propellant Options for High-Power Hall Thrusters," *Proceedings of the Space Nuclear Conference*, San Diego, CA, 2005, Paper 1092.

[4] Dressler, R., Chiu, Y., and Levandier, D., "Propellant Alternatives for Ion and Hall Effect Thrusters," *AIAA*-2000-062, 2000.

[5] Robert S. Jankovsky, David H. Manzella, and Richard R. Hofer, "NASA's Hall Thruster Program," in *37th AIAA Joint Propulsion Conference*, Salt Lake City, 2001, pp. 1-14.

[6] Busek Co. Inc. (2006) Buesk Co. Inc. - Hall Effect Thrusters. [online database]. http://www.busek.com/halleffect.html [cited 1 Mar 2011].

[7] R. L. Sackheim and D.C. Byers, "Status and Issues Related to In-Space Propulsion Systems," *Journal of Propulsion and Power*, vol. 14, no. 5, pp. 669-675, September-October 1998.

[8] Goebel, D., Katz, I., "*Fundamentals of Electric Propulsion: Ion and Hall Thrusters*," 1st ed. Hoboken, NJ: John Wiley & Sons, 2008.

[9] Richard R. Hofer, Lee K. Johnson, Dan M. Goebel, and Dennis J. Fitzgerald, "Effects of an Internally-Mounted Cathode on Hall Thruster Plume Properties," in *42nd AIAA/ASME/SAE/ASEE Joint Propulsion Conference and Exhibit*, Sacramento, 2006, pp. 1-23.

[10] Massey, D., King, L. "Progress on the Development of a Direct Evaporation Bismuth Hall Thruster," *Joint Propulsion Conference*, July 2005.

[11] Rotter, J.E., *An Analysis of Multiple Configurations of Next-Generation Cathodes in a Low Power Hall Thruster*, Master's Thesis, March 2009.

[12] Kim, V., "Main Physical Features and Processes Determining the Performance of Stationary Plasma Thrusters," *Journal of Propulsion and Power*, vol. 14, no. 5, pp. 736-743, September-October 1998.

[13] Haag, T., "Design of a Thrust Stand for High Power Electric Propulsion Devices," AIAA-89-2829, *25th Joint Propulsion Conference*, Monterey, CA, July 10-12, 1989.

[14] Temkin, S. E., *Performance Characterization of a Three-Axis Hall Thruster*, Master's Thesis, December 2010.

[15] Azziz, Y., "Experimental and Theoretical Characterization of a Hall Thruster Plume," Ph. D. Dissertation, Department of Aeronautics and Astronautics, Massachusetts Institute of Technology, Boston, MA, 2007.

[16] Walker, M., Hofer, R. and Gallimore, A., "The Effects of Nude Faraday Probe Design and Vacuum Facility Backpressure on the Measured Ion Current Density Profile of Hall Thruster Plumes," AIAA 2002-4253, *38th AIAA Joint Propulsion Conference*, Indianapolis, IN, July 7-10, 2002.

[17] Azziz, Y., Martinez-Sanchez, M., Szabo, J., "Determination of In-Orbit Plume Characteristics from Laboratory Measurements," AIAA-2006-4484, 42nd AIAA Joint Propulsion Conference, Sacramento, California, July 9-12, 2006.

[18] Shastry, R., Hofer, R. R., Reid, B. M., Gallimore, A. D., "Method for Analyzing ExB Probe Spectra from Hall Thruster Plumes," Proceedings of the 44th AIAA Joint Propulsion Conference, AIAA-2008-4647, Hartford, CT, July 20-23, 2008.

[19] Casey Farnell and John D. Williams, "ExB Probe Operating Manual," Colorado State Univeristy, Ft. Collins, Instrument Manual 2007.

[20] Hofer, R. R., Gallimore, A. D., "Ion Species Fractions in the Far-Field Plume of a High-Specific Impulse Hall Thruster," AIAA-2003-5001, 39th Joint Propulsion Conference, Huntsville, AL, July 20-23, 2003.

[21] "Iodine." *NIST WebBook*. Web. 01 Feb. 2011. [online database]. http://webbook.nist.gov/cgi/cbook.cgi?Formula=i2&NoIon=on&Units=SI [cited 1 Mar 2011].

REPORT DOCUMENTATION PAGE

Form Approved
OMB No. 074-0188

1. REPORT DATE *(DD-MM-YYYY)*	**2. REPORT TYPE**	**3. DATES COVERED** *(From – To)*
24-03-2011	Master's Thesis	Sep 2009 – March 2011

4. TITLE AND SUBTITLE

Revolutionizing Space Propulsion Through The Characterization Of Iodine as Fuel For Hall-Effect Thrusters

5a. CONTRACT NUMBER

5b. GRANT NUMBER

5c. PROGRAM ELEMENT NUMBER

6. AUTHOR(S)

Hillier, Adam C., 2nd Lt, USAF

5d. PROJECT NUMBER
11Y133

5e. TASK NUMBER

5f. WORK UNIT NUMBER

7. PERFORMING ORGANIZATION NAMES(S) AND ADDRESS(S)
Air Force Institute of Technology
Graduate School of Engineering and Management (AFIT/ENY)
2950 Hobson Way, Building 640
WPAFB OH 45433-8865

8. PERFORMING ORGANIZATION REPORT NUMBER
AFIT/GA/ENY/11-M08

9. SPONSORING/MONITORING AGENCY NAME(S) AND ADDRESS(ES)
Michael T. Huggins, Air Force Research Lab, Space and Missile Propulsion Division
5 Pollux Drive, Bldg 3353
Edwards AFB, CA 93524
DSN 525-5230 Comm. 661-275-5230

10. SPONSOR/MONITOR'S ACRONYM(S)
AFRL/RZS

11. SPONSOR/MONITOR'S REPORT NUMBER(S)

12. DISTRIBUTION/AVAILABILITY STATEMENT

APPROVED FOR PUBLIC RELEASE; DISTRIBUTION UNLIMITED.

13. SUPPLEMENTARY NOTES

14. ABSTRACT

The demand for increased performance in space propulsion systems is higher than ever as missions are becoming more advanced. As the global supply of xenon depletes, missions demanding high thrust will require alternatives. The research presented here examines iodine as an alternate propellant. The propellant was successfully operated through a BHT-200 thruster in the T6 vacuum facility at Busek Co. Inc. A feed system for the iodine was developed for controlled thruster operation at varying conditions. An inverted pendulum was used to take thrust measurements. Thrust to power ratio, anode efficiency, and specific impulse were calculated. Iodine performance is compared to xenon. Plume measurements were taken by a nude Faraday probe, which measured current density, and an ExB probe, also known as a Wein filter, which measured individual species properties. The data validated anode efficiency from performance measurements. Plume comparisons were made between iodine and xenon. Iodine was found to perform similarly to xenon, but with superior performance at high voltage. Possible effects of iodine operation on spacecraft, thrusters, and power systems were explored.

15. SUBJECT TERMS

Hall Effect Thrusters, Space Propulsion, Thruster Performance, Propellant

16. SECURITY CLASSIFICATION OF:			**17. LIMITATION OF ABSTRACT**	**18. NUMBER OF PAGES**	**19a. NAME OF RESPONSIBLE PERSON**
a. REPORT	**b. ABSTRACT**	**c. THIS PAGE**			Richard E. Huffman, Lt Col, USAF
U	**U**	**U**	**UU**	87	**19b. TELEPHONE NUMBER** *(Include area code)* (937) 255-3636, ext 7490

Standard Form 298 (Rev. 8-98)
Prescribed by ANSI Std. Z39-18